

Characterization of LPBF 316 for Structural Applications in Nuclear

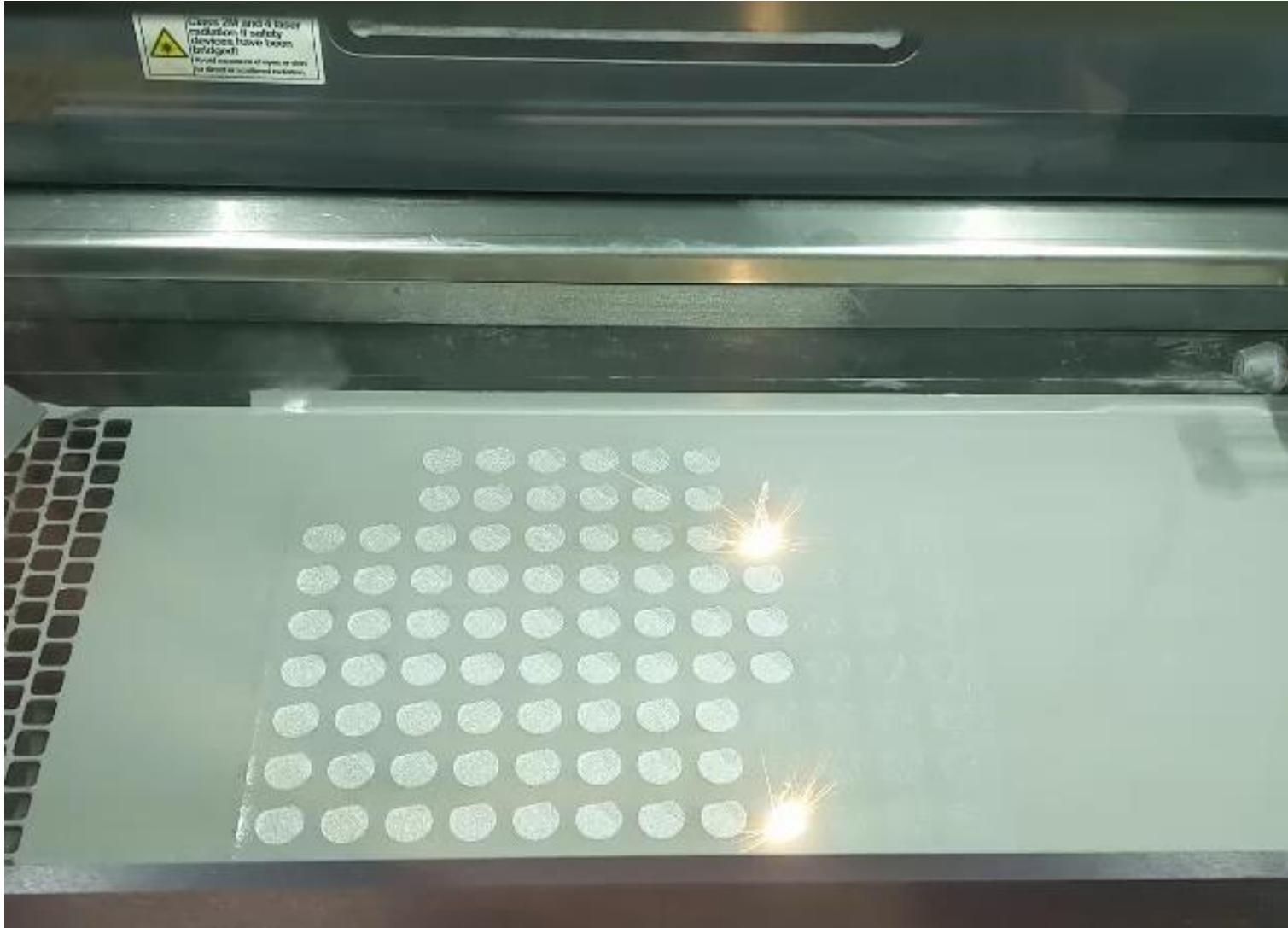
Advanced Materials & Manufacturing Technologies (AMMT) Program Review

May 18, 2022

Ryan Dehoff¹, Bogdan Alexandreanu², Xuan Zhang², Yiren Chen², TS Byun¹, Kory Linton¹, Caleb Massey¹

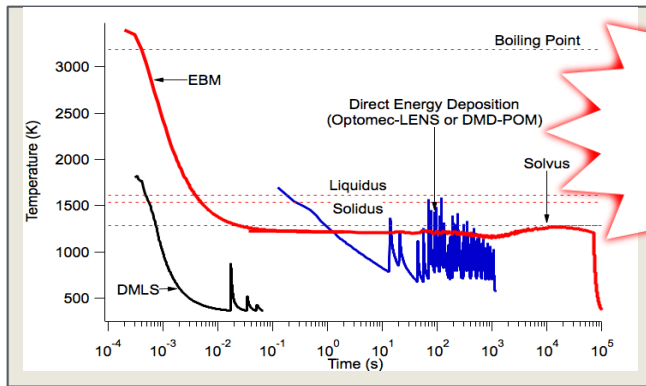
1. Oak Ridge National Laboratory
2. Argonne National Laboratory

Laser Powder Bed Additive Manufacturing



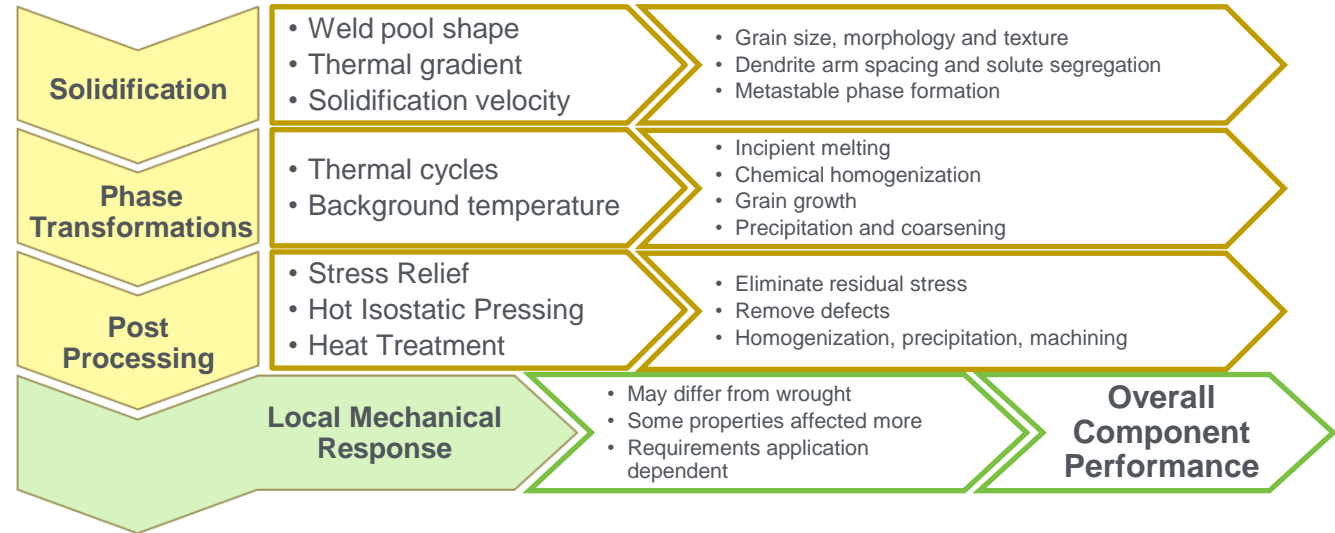
Metal Additive Manufacturing

Complex thermal cycles directly influence key materials properties

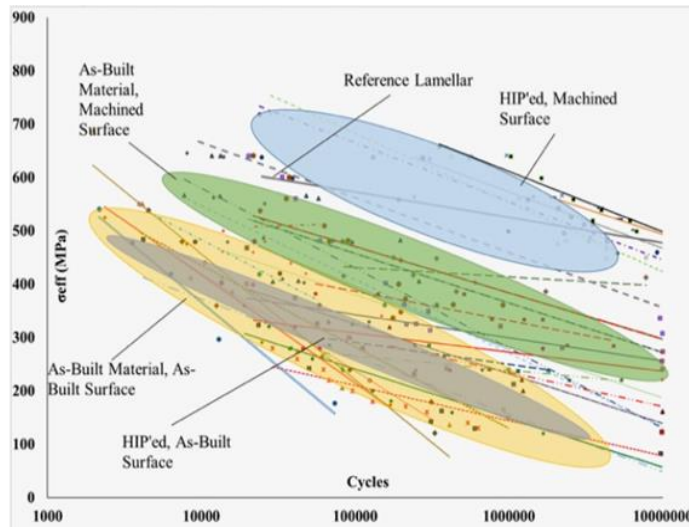


Each Geometry has a different Thermal Signature

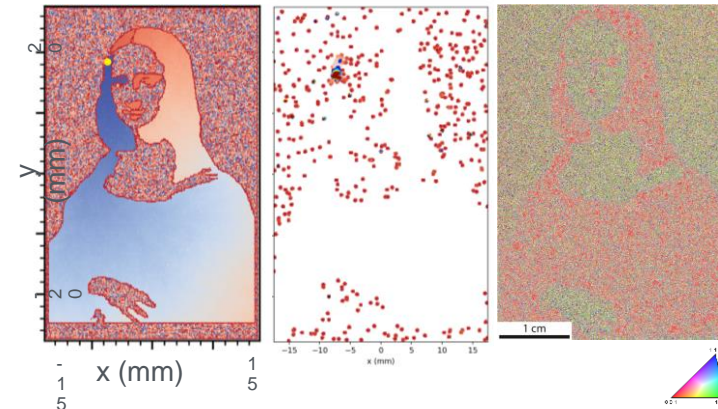
Key variables: Process conditions, material properties, *geometry*, scan pattern



Variation of Mechanical Performance in AM Literature



Scan path optimization enables detailed control over the spatial distribution of grain texture



Objective

- To develop and qualify additively manufactured (AM) structural materials in support of a broad range of nuclear reactor types
- Preliminary development and testing at ANL and ORNL

Reactor categories	Design and operation needs
LWRs (incl. LWR-type SMRs)	Tensile, fatigue, fracture toughness, thermal aging, SCC, environmental fatigue, irradiation, weldability and weld integrity
Advanced high-T reactors	Tensile properties, high-temperature time-dependent aging effects (e.g. creep and creep-fatigue), thermal aging, irradiation and corrosion effects, weldability and weld integrity

* US NRC, Draft Guidelines Document for Additive Manufacturing—Laser Powder Bed Fusion, ML21074A

Performance of 316L Stainless Steel for Structural Applications: Post-irradiation Behavior

T.S. Byun

Manufacturing of Materials: R.R. Dehoff, A.M. Rossy, C.B. Joslin, K.K. Carver

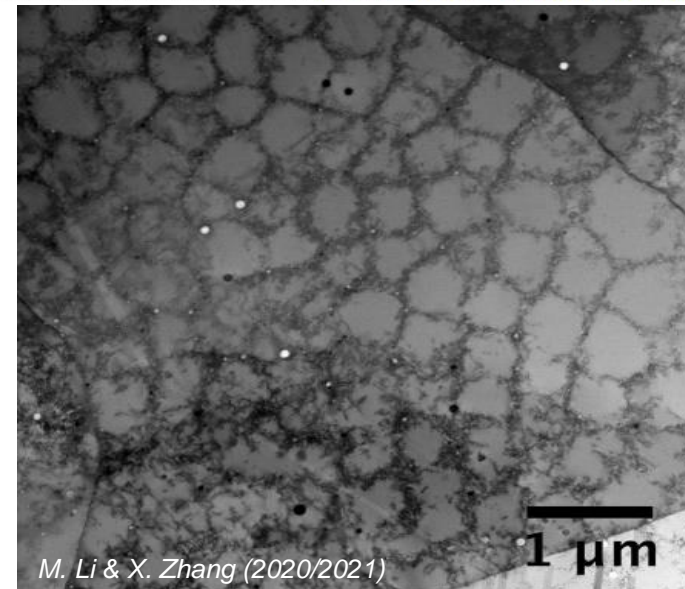
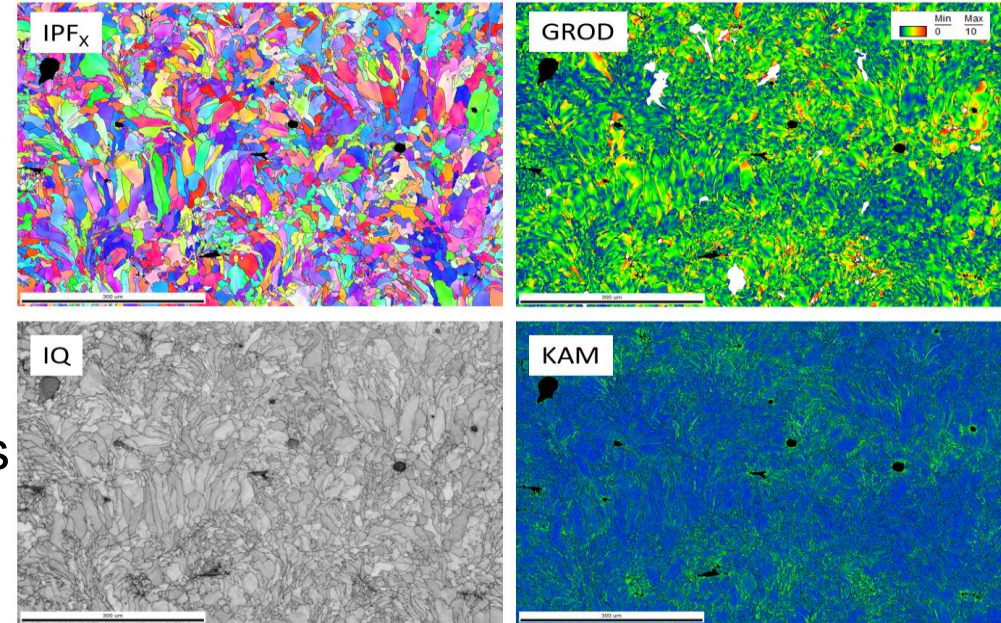
Irradiation/Characterization/PIE: A. Le Coq, K. Linton, M.N. Gussev, B.E.

Garrison, X. Chen, T.G. Lach

Oak Ridge National Laboratory

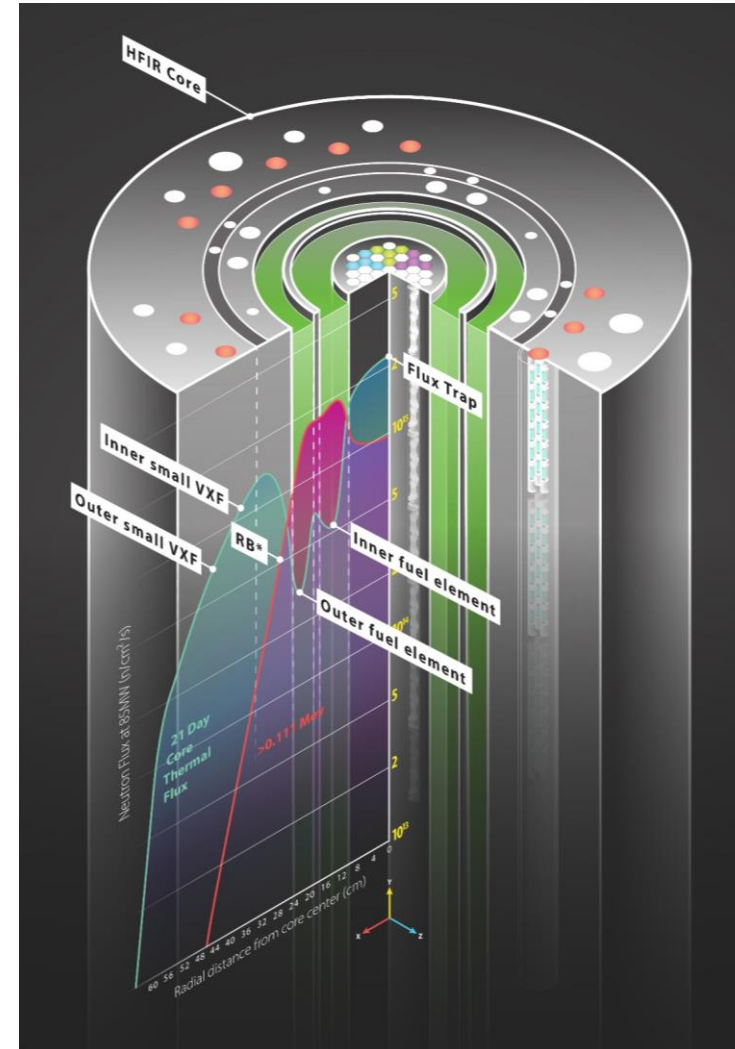
Introduction

- AM 316L alloy has a unique microstructure, including high-density dislocation network and ultrafine grain structure, and thus different properties compared to those produced via traditional processing routes.
- Response of the AM alloys to neutron irradiation is the main gap in the current knowledge base for nuclear applications.
- This work scope aims to demonstrate the in-reactor capabilities of the AM 316L and other core materials (AM IN 718 & SiC).
- *Report on the status of irradiation experiment and post-irradiation evaluation.*
- *Discuss the mechanical behavior of AM316L and Wrought (WT) 316L stainless steels before and after neutron irradiation to 2 dpa.*



High Flux Isotope Reactor

- HFIR flux trap provides up to 1.9×10^{15} neutrons/cm²/sec (>0.111 Mev)
- Constant 85 MW power, ~24 days per cycle, six to seven cycles per year
- Using flux trap with previously designed irradiation vehicles (known as “rabbit” capsules) allows for accelerated testing
- For the program:
 - 24 rabbits completed HFIR irradiation (includes 316L, IN 718, YHx, and SiC capsules)
 - 8 rabbits inserted in HFIR flux trap
 - 3 rabbits being prepared for HFIR irradiation



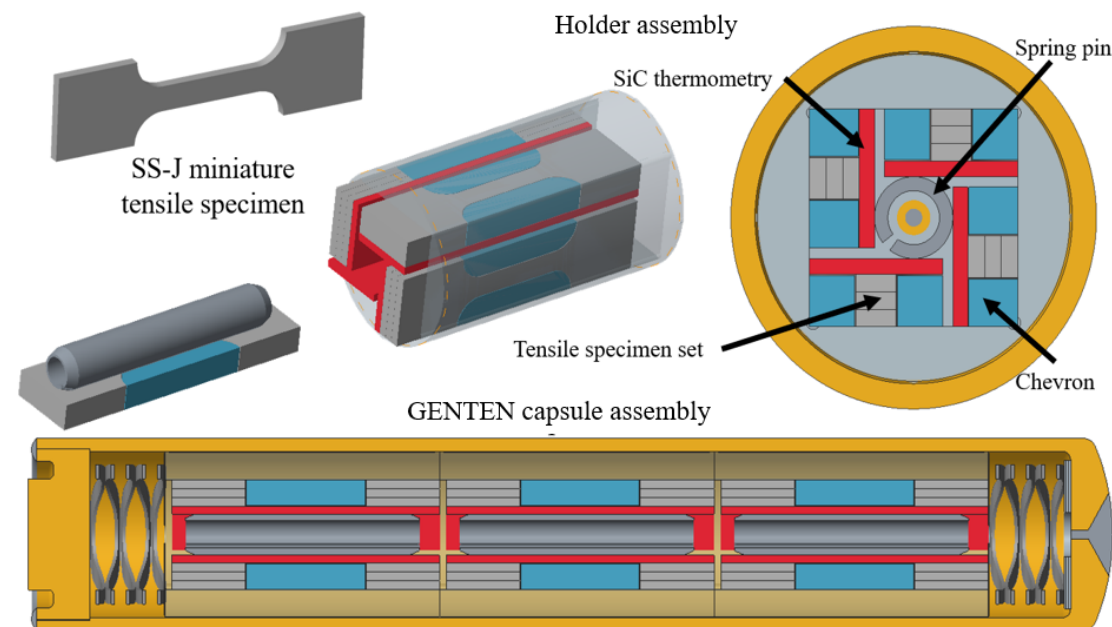
HFIR core cutout with fast and thermal flux axial profile

316L SS and Inconel 718 Irradiation Experiment

FY	Capsule ID	Irradiation temperature (°C)	Dose (dpa)	Specimen
FY 20	GTCR01	300	0.2	36 SSJ2 (316L)
	GTCR02	300	2	As-printed, heat-treated, wrought
	GTCR03	300	8	
	GTCR04	600	0.2	
	GTCR05	600	2	
	GTCR06	600	8	
FY 21	GTCR07	300	2	
	GTCR08	600	2	8 SSJ3 (316L)+ 24 SSJ2 (Inconel 718)
	GTCR09	300	10	
	GTCR10	600	10	
	GTCR11	300	2	
	GTCR12	600	2	
	GTCR13	300	10	
	GTCR14	600	10	

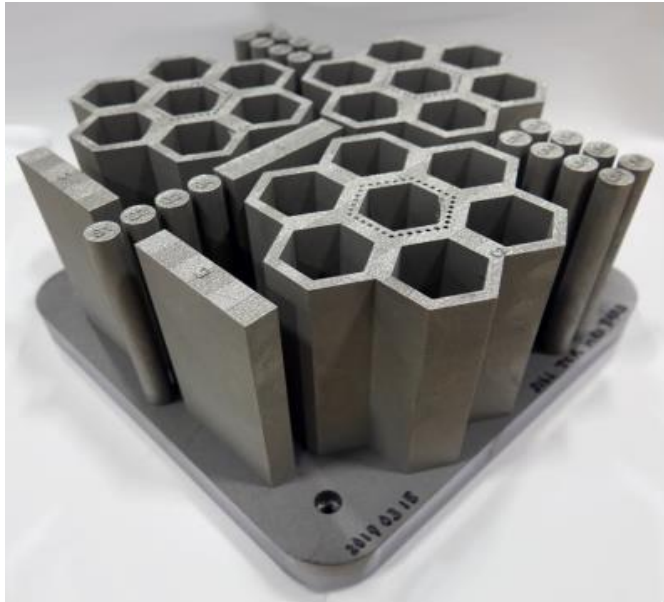
FY21 irradiation campaign:

- Eight capsules
- Two temperatures, two doses
- Tensile specimens
 - 316L SS: SSJ3 (0.75 mm-thick)
 - Inconel 718: SSJ2 (0.5 mm thick)



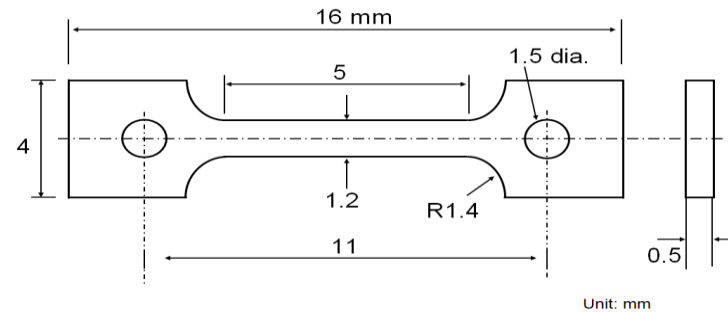
P. A. Champlin et al., "Capsule and Specimen Geometries for HFIR Irradiation Testing Supporting the Transformational Challenge Reactor," ORNL/TM-2019/1310, Oak Ridge National Laboratory, Oak Ridge, Tennessee, 2019.

316L SS by LPBF and Reference 316L



316L	Fe	Cr	Ni	Mo	Mn	Si	N	Cu	Co	C	P	O
AM 316L (Praxair powder)	Bal.	17.1	12.1	2.41	1.19	0.46	0.01	0.01	0.1	0.006	<0.005	0.05
WT 316L (Wrought)	Bal.	16.7	10.2	2.03	0.63	0.53	0.04 7	-	-	-	0.027	-

SS-J2 Tensile Specimen



❑ *Machining of SS-J2 miniature tensile specimens from an additively manufactured plate (AM 316L) and a bulk material bar (WT 316L).*

- ❑ **AM 316L as-built**
- ❑ **AM 316L stress-relieved (650 ° C/1h)**
- ❑ **AM 316L solution-annealed (1050 ° C/1h)**
- ❑ **WT 316L solution-annealed (~1040 ° C)**

316L SS and Inconel-718 Irradiation Experiment

❑ AM 316L SS specimens (effect of local AM microstructure)

❑ 6 conditions:

1.5-mm thick plate:

- Center layers

5-mm thick plate:

- Center layers
- Surface layers

40-mm cube:

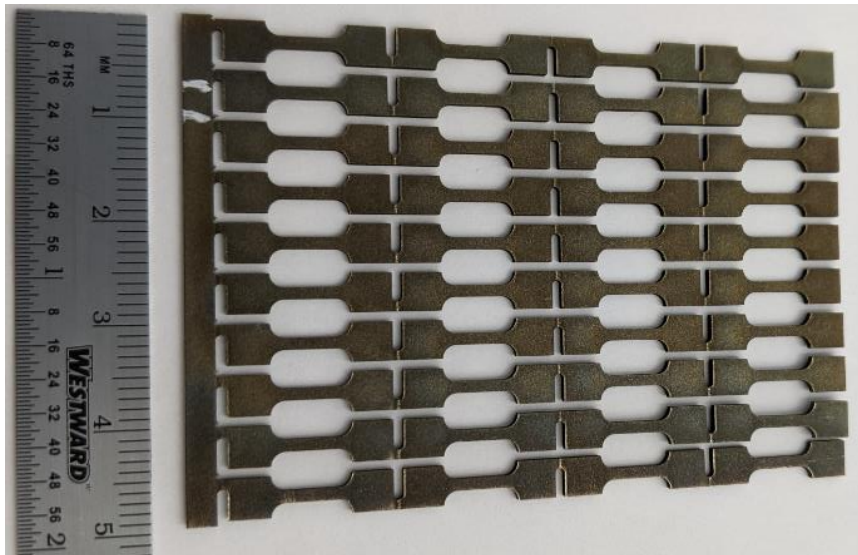
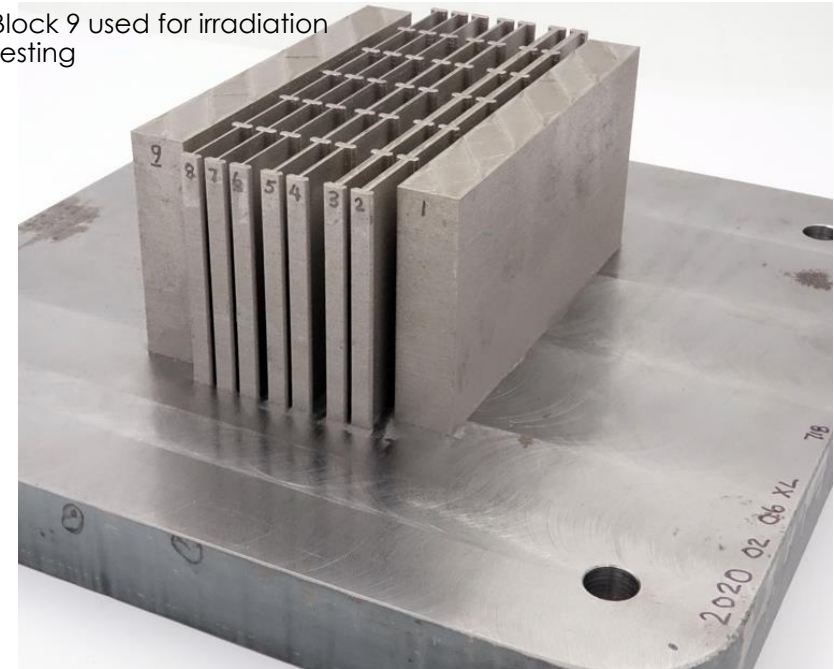
- Surface layers
- 10-mm from edge
- Center layers

❑ Inconel-718 specimens: 4 conditions

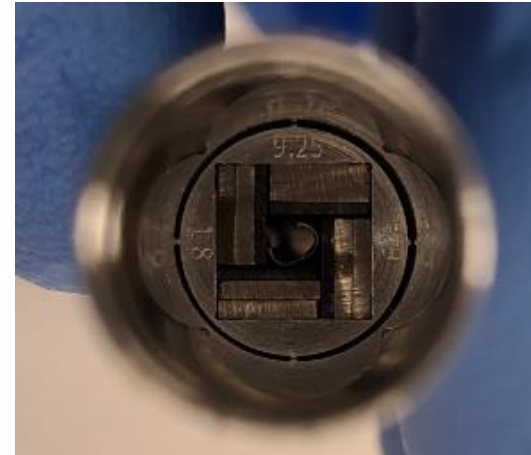
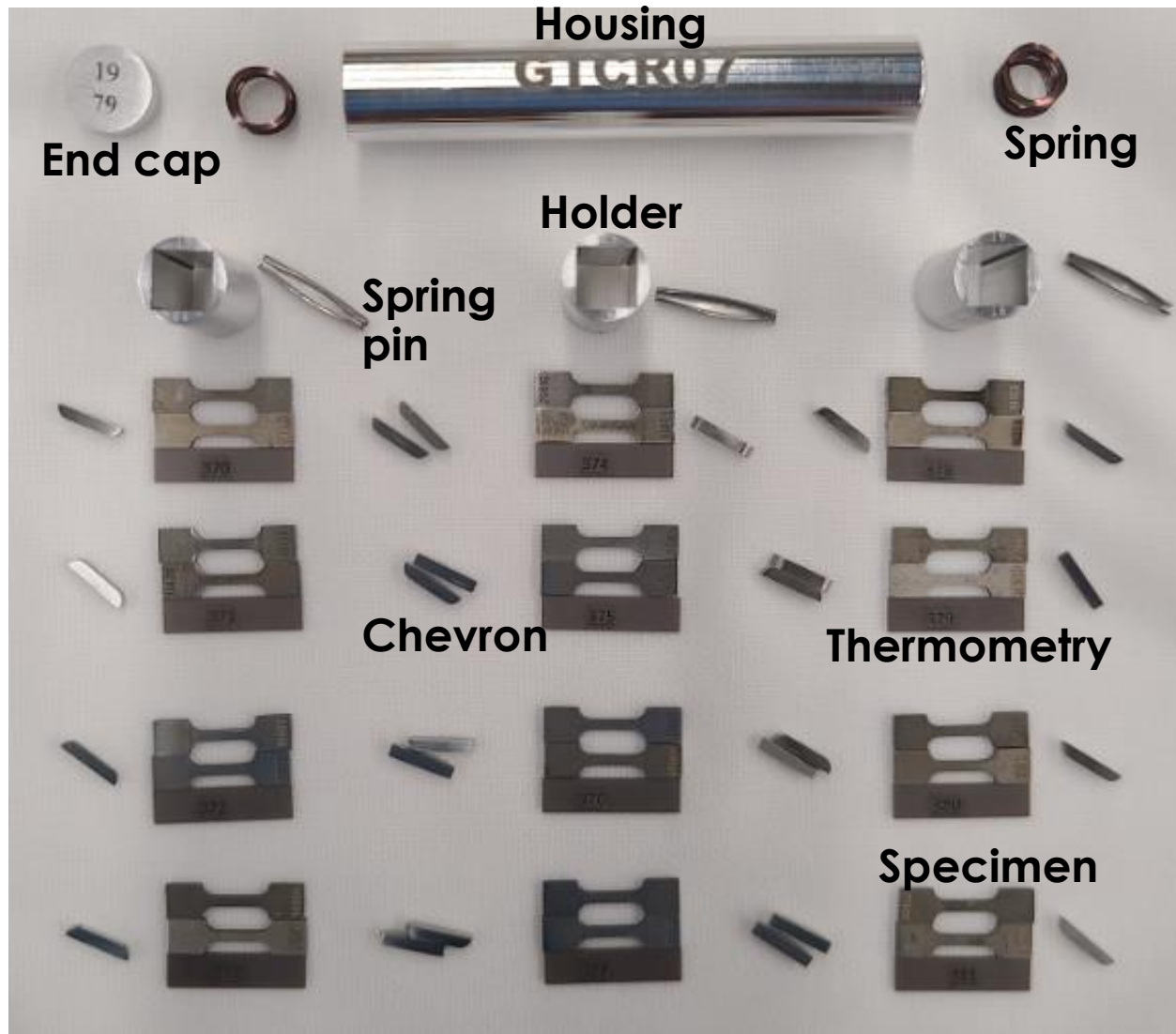
- Wrought, with ASTM heat treatment
- AM, with 3 different heat treatment



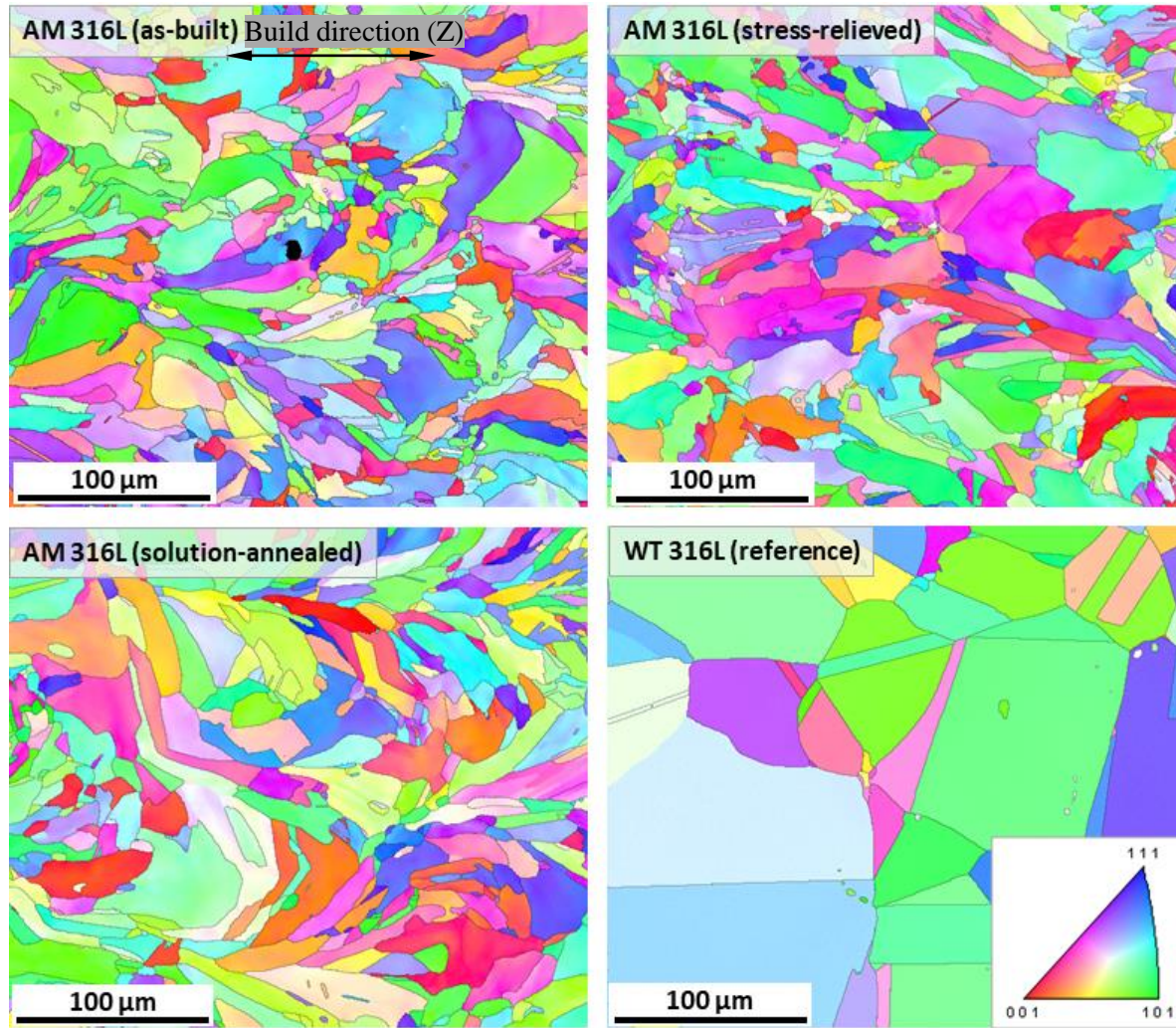
Block 9 used for irradiation testing



Capsule Assembly for 316L SS and Inconel-718 Irradiation



Grain Structures of AM 316L SS in Three Conditions and WT 316L SS



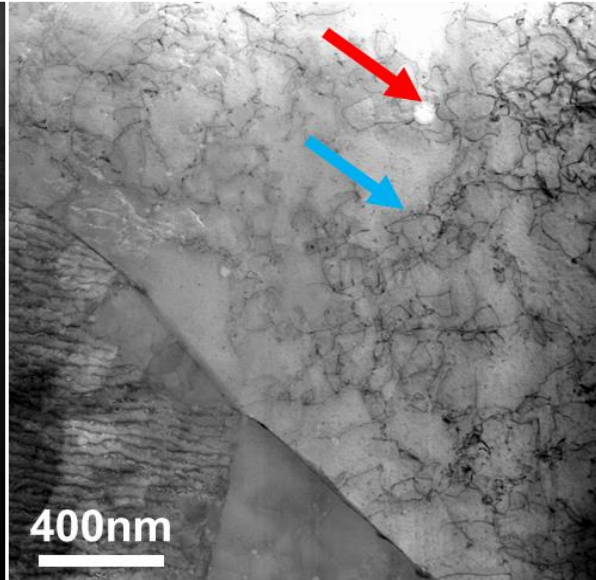
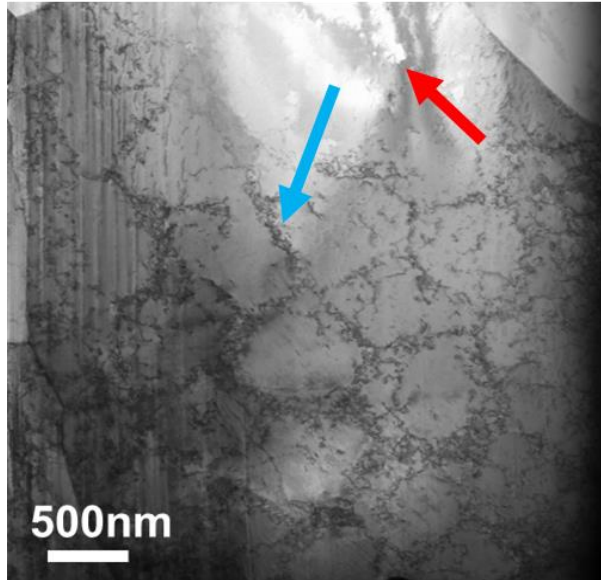
- The AM 316L SS in the as-built condition has a very fine microstructure, with mostly irregularly bent or crescent-shaped fine grains; there are the remnants of the melting pools, which are partially remelted and reheated multiple times by subsequent laser beam passes.
- Neither of the post-build annealing treatments at 650 °C and 1,050 °C caused apparent grain growth; the average intercept lengths of grain boundaries were measured at 13–15 μm.
- Such unique grain structures are contrasted to that of the wrought 316L steel, which has much larger (~47 μm on average) and equiaxed grains with many straight grain or twin boundaries.

Fig - Microstructures (EBSD IPF maps) of AM 316L in as-built, stress-relieved, and solution-annealed conditions, where the build direction (Z) is horizontal. The EBSD IPF maps are colored relative to the building (horizontal) direction. The reference 316L is in solution-annealed condition.

Grain Structures of AM 316L and WT 316L Stainless Steels

(a) As-built

(b) 650 °C Stress Relieved



(c) 1050 °C Solution Annealed

(d) Reference Wrought

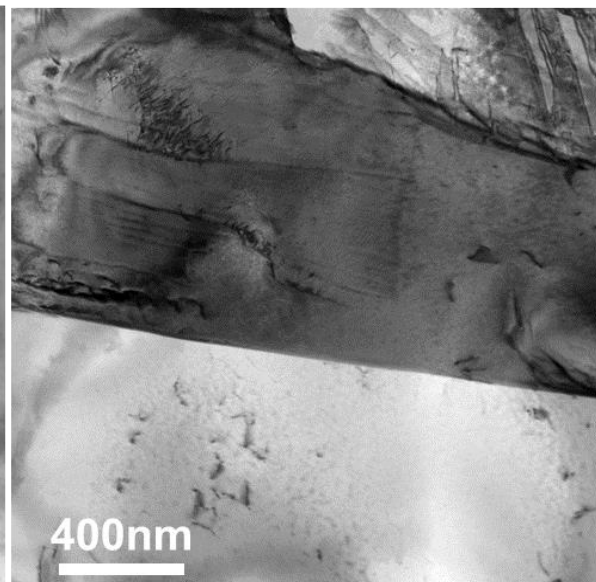
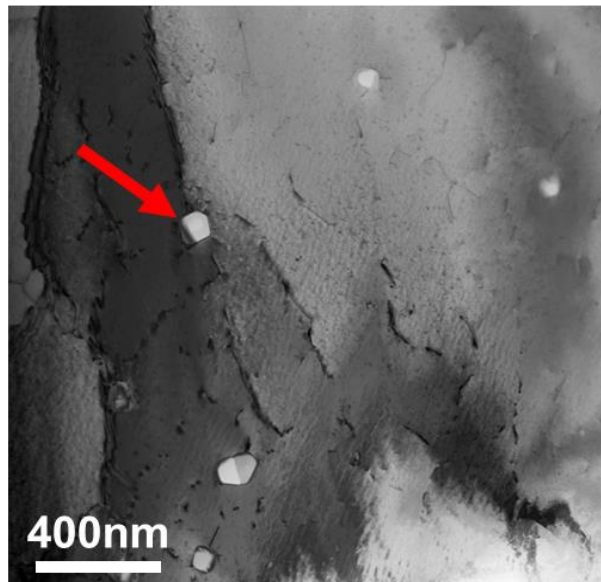


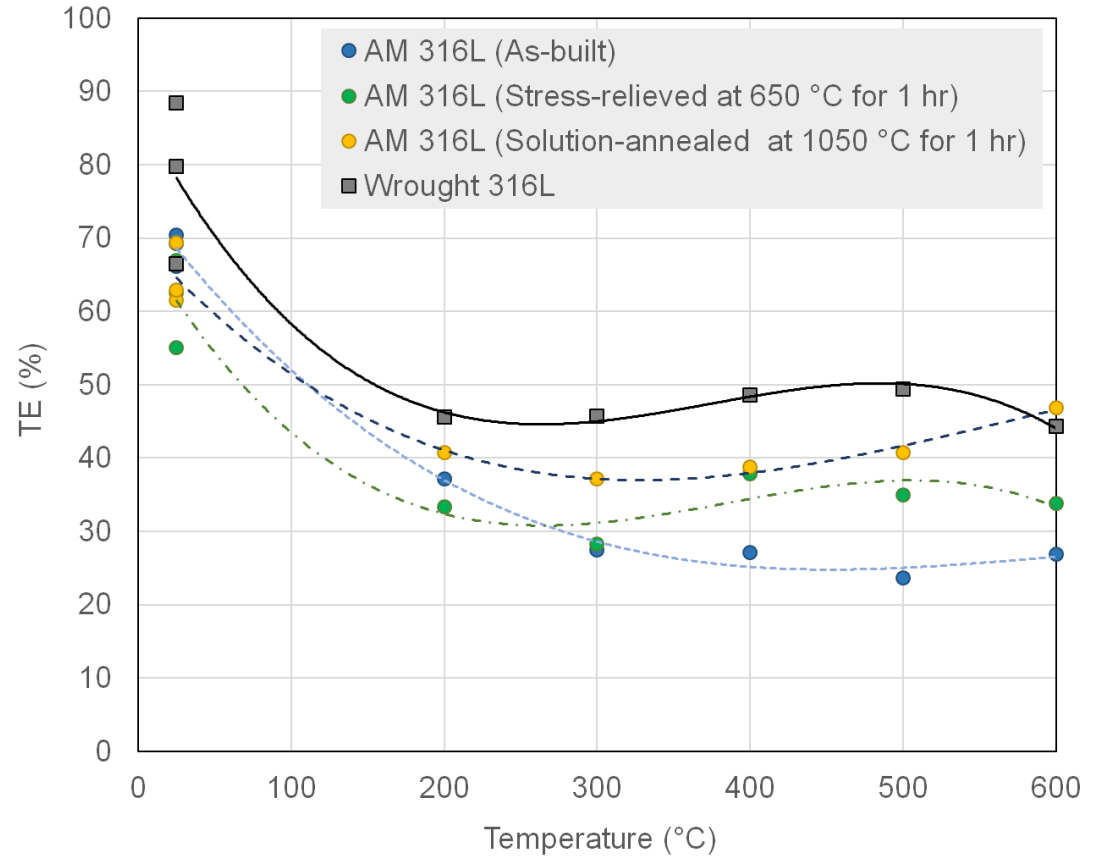
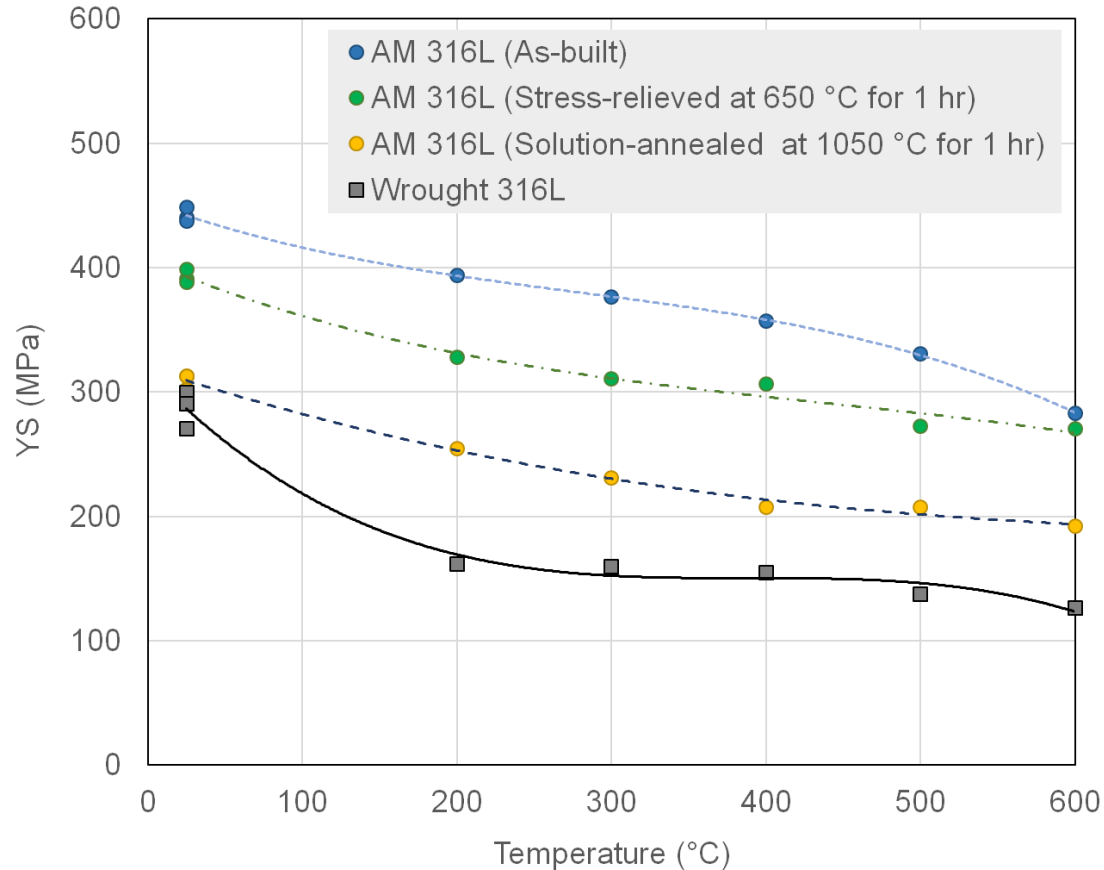
Fig - STEM BF micrographs of AM 316L SS in (a) as-built, (b) stress-relieved, and (c) solution-annealed conditions. Panel (d) shows the reference WT 316L SS.

Blue arrows - dislocation cellular structures

Red arrows - oxide inclusions in the AM steel.

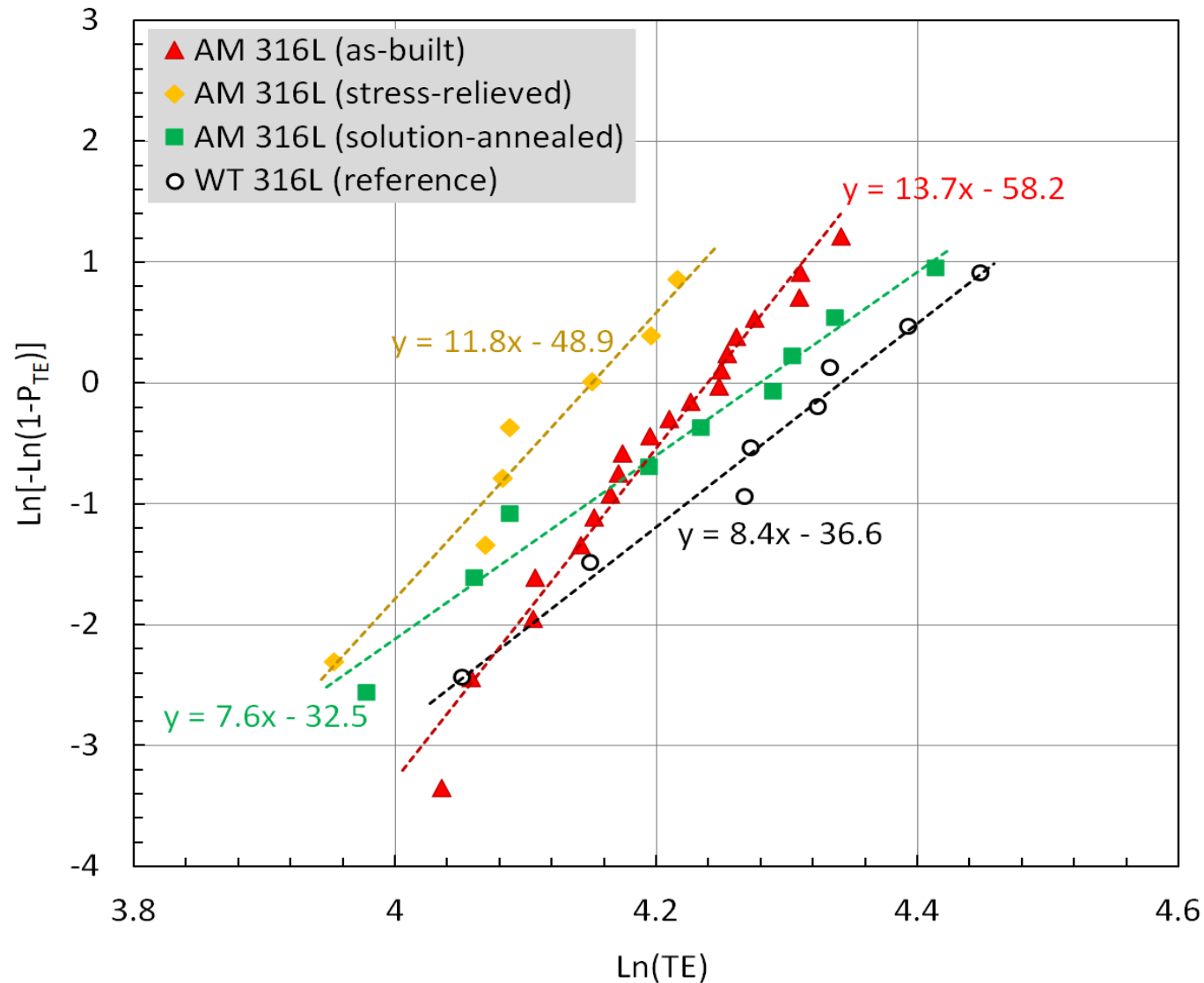
Note - the reference material in (d) has neither cells nor oxide inclusions.

Tensile Properties of 316L: Baseline Strength & Ductility



- Yield strength (YS) data show significant differences among the AM and wrought 316L steels.
- Lower ductility (TE) was measured from in the AM 316L; the lowest uniform ductility is ~20%, which is measured from the as-built 316L.
- The variation of mechanical properties among the 316L materials becomes less significant in the later part of deformation.

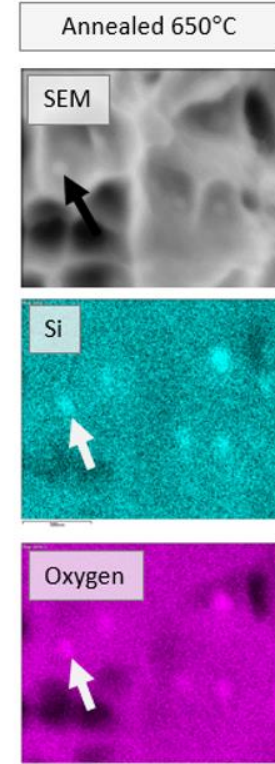
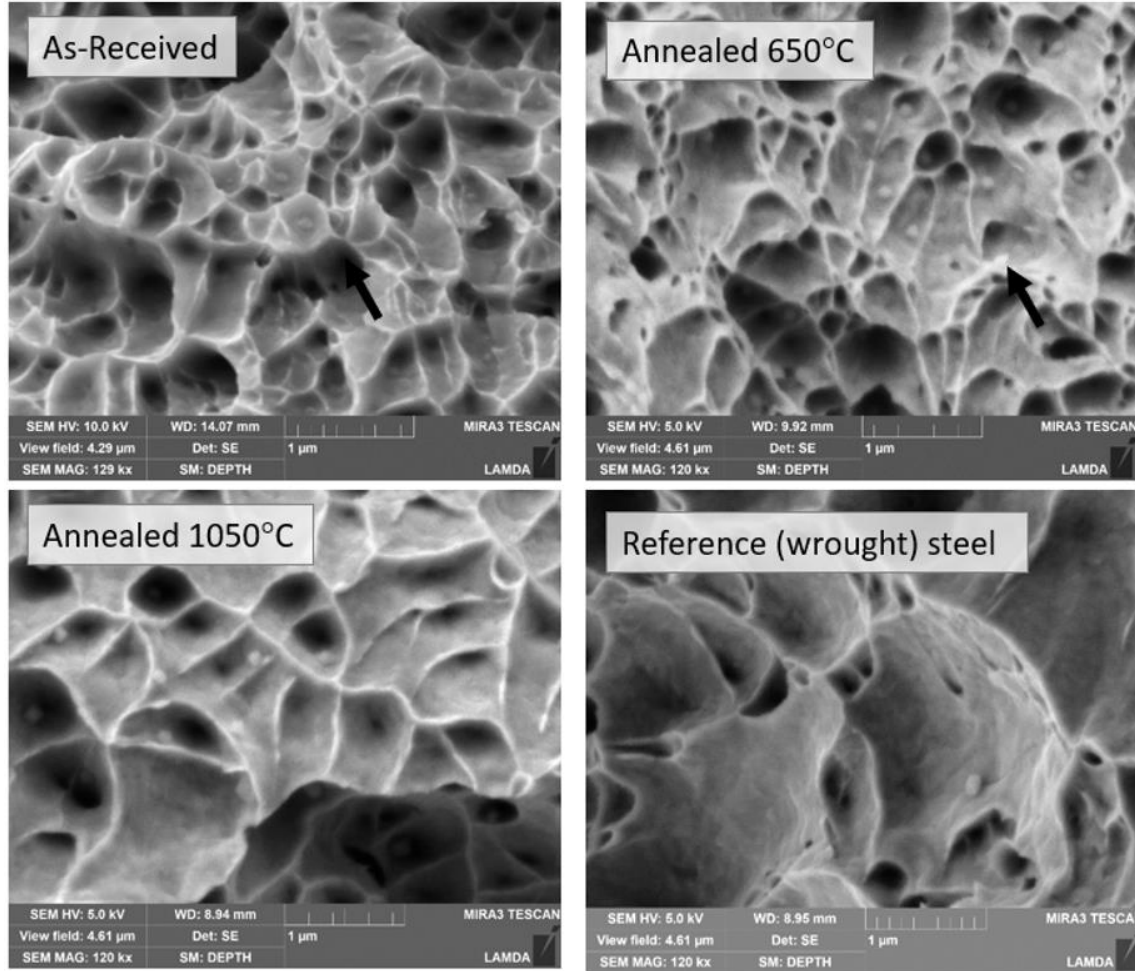
Tensile Properties of 316L: Statistical Behavior



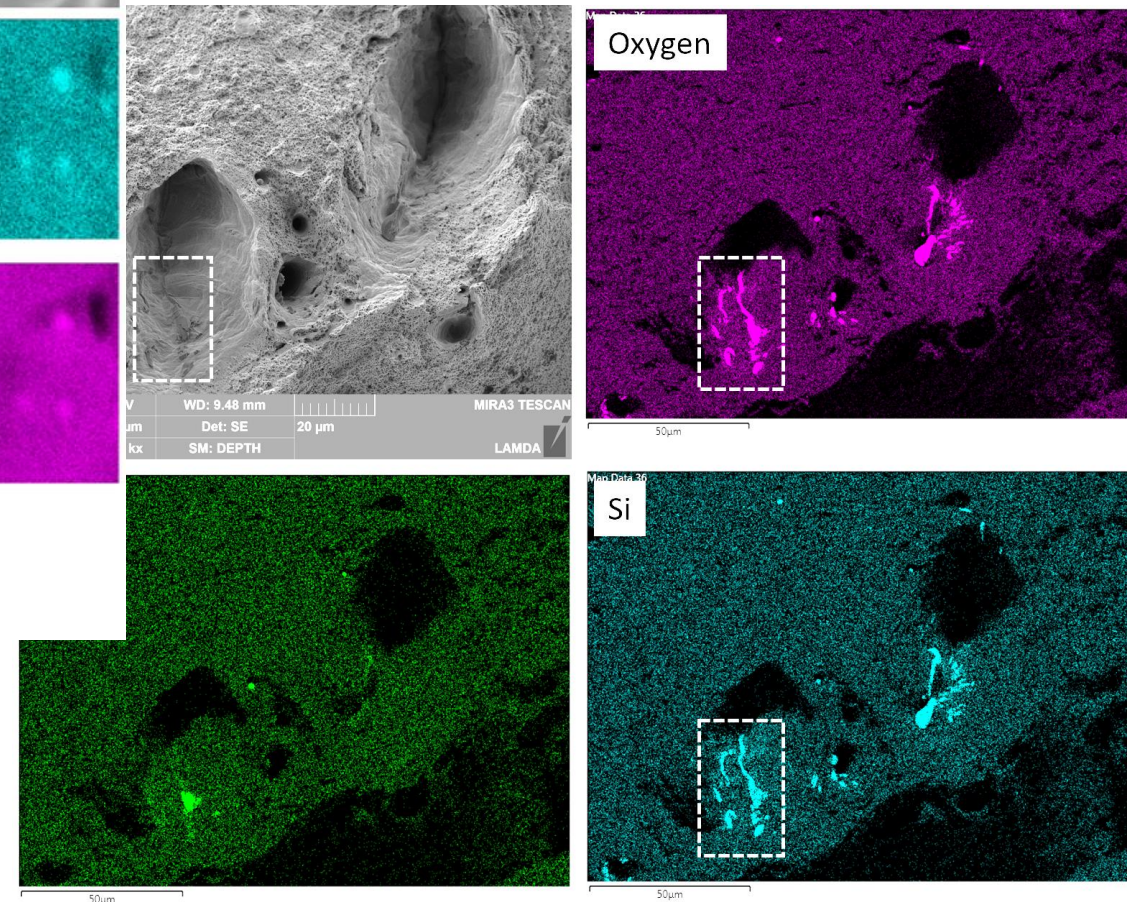
- Contrary to the expectation that the AM materials may show higher variations in their properties, the TE data of AM 316L SS in as-built condition shows the highest Weibull modulus.
- The combination of very fine microstructure and high residual stress on a such small scale may lead to more uniform deformation.
- Other strength and ductility parameters (YS, UTS, UE) also show similar statistical behaviors.

Fig - Weibull plots for total elongation (TE) data of 316L SSs in four different conditions.

Tensile Properties of AM and WT 316L SSs: Fracture Surfaces

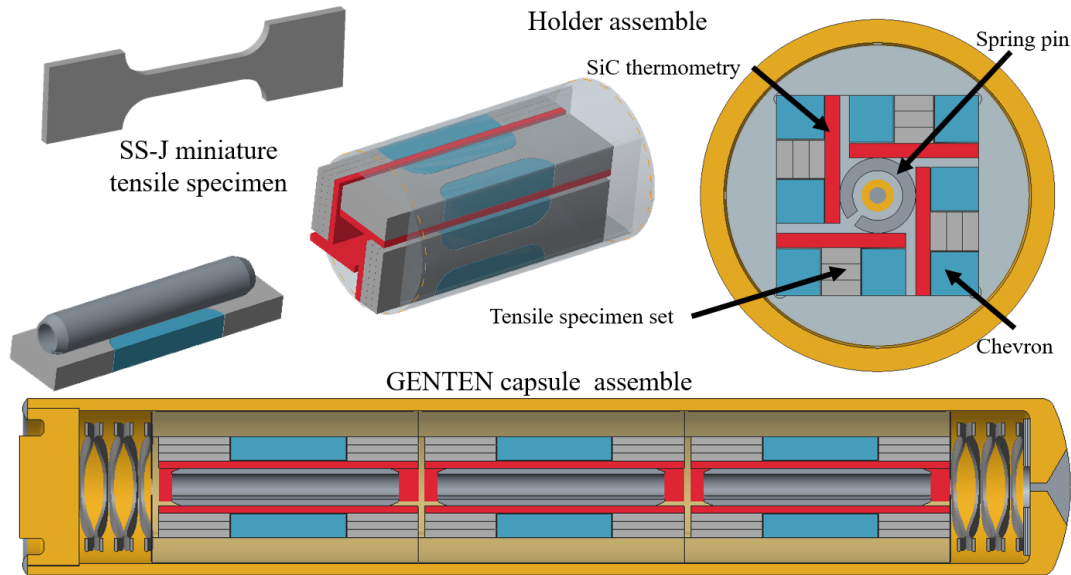


A fracture surface of as-built AM 316L steel in which two mesoscale pores are overlapped with EDS maps (oxygen, aluminum, and silicon). ↓



Fracture surfaces of the AM 316L and WT 316L specimens: the ductile fracture, dimple coalescence mechanism is commonly observed but with different dimple sizes.

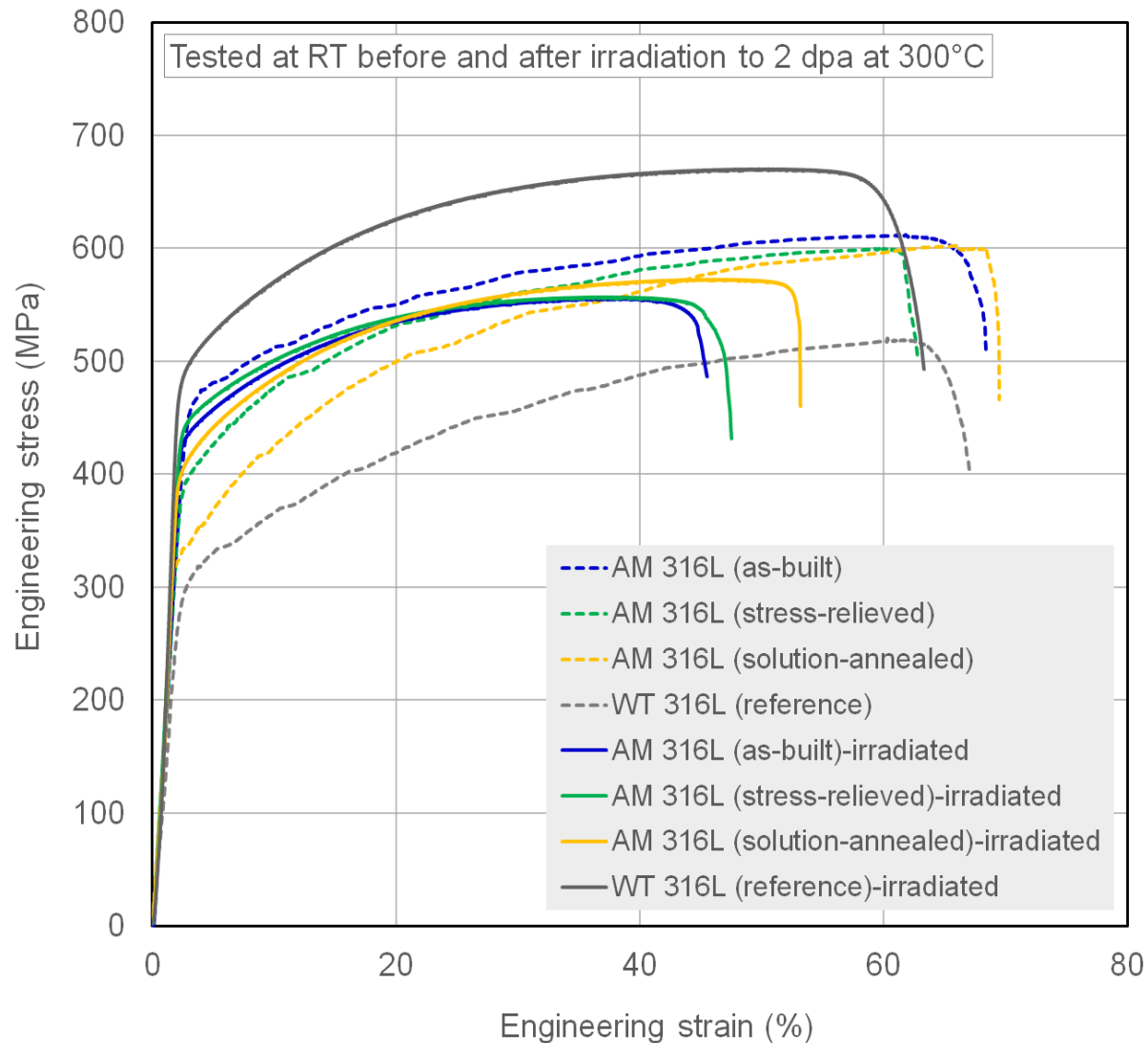
HFIR Irradiation of AM 316L and WT 316L Tensile Specimens & PIE



Capsule	Target Temp.	Dose (dpa)	TM Temp. (°C)	σ	Sample Temp. (°C)	Note
GTCR01	300°C	0.2	265	4°C	~250	PIE
GTCR02	300°C	2	391	25°C	~380	PIE
GTCR03	300°C	8				Irradiation Continued
GTCR04	580°C	0.2	688	45°C	~670	PIE
GTCR05	600°C	2	615	11°C	~600	PIE
GTCR06	600°C	8				Irradiation Continued

- ❑ 216 SS-J2 tensile specimens have been loaded in 6 rabbit capsules.
- ❑ Post-irradiation tensile tests have been performed for selected conditions: 32 tests completed; 20 tests on going.
- ❑ ***Tensile testing was performed at RT, 300°C and 500°C. Results are discussed.***

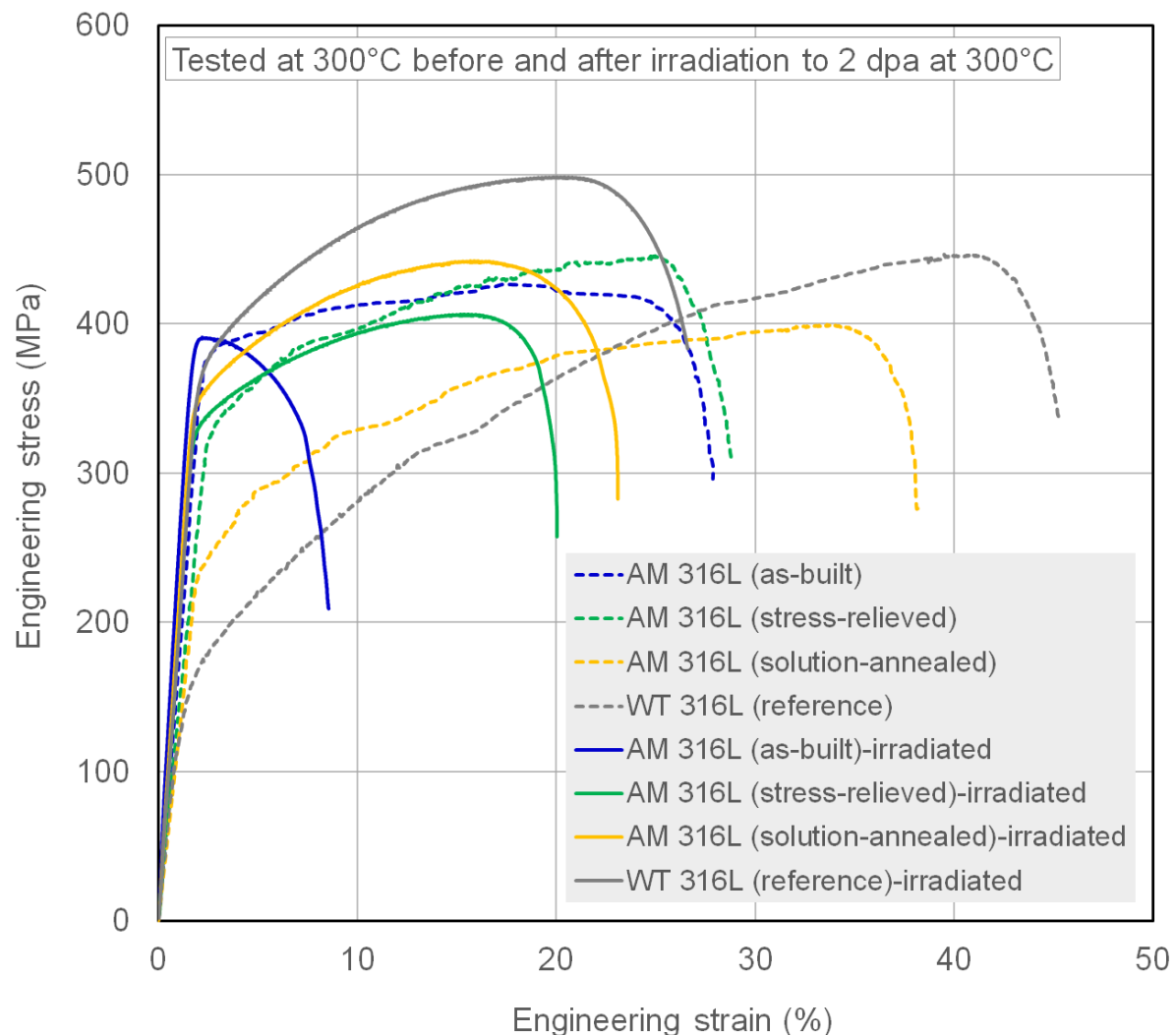
AM 316L and WT 316L after Irradiation: Tensile Curves at RT



Engineering stress-strain curves of AM 316L in as-built, stress-relieved, and solution annealed conditions and wrought 316L tested at RT after irradiation to 2 dpa at 300°C.

- *WT 316L shows the lowest irradiation hardening, with a small reduction of ductility.*
- *Smaller strength changes are observed with higher strength AM materials, but with larger reduction of ductility.*

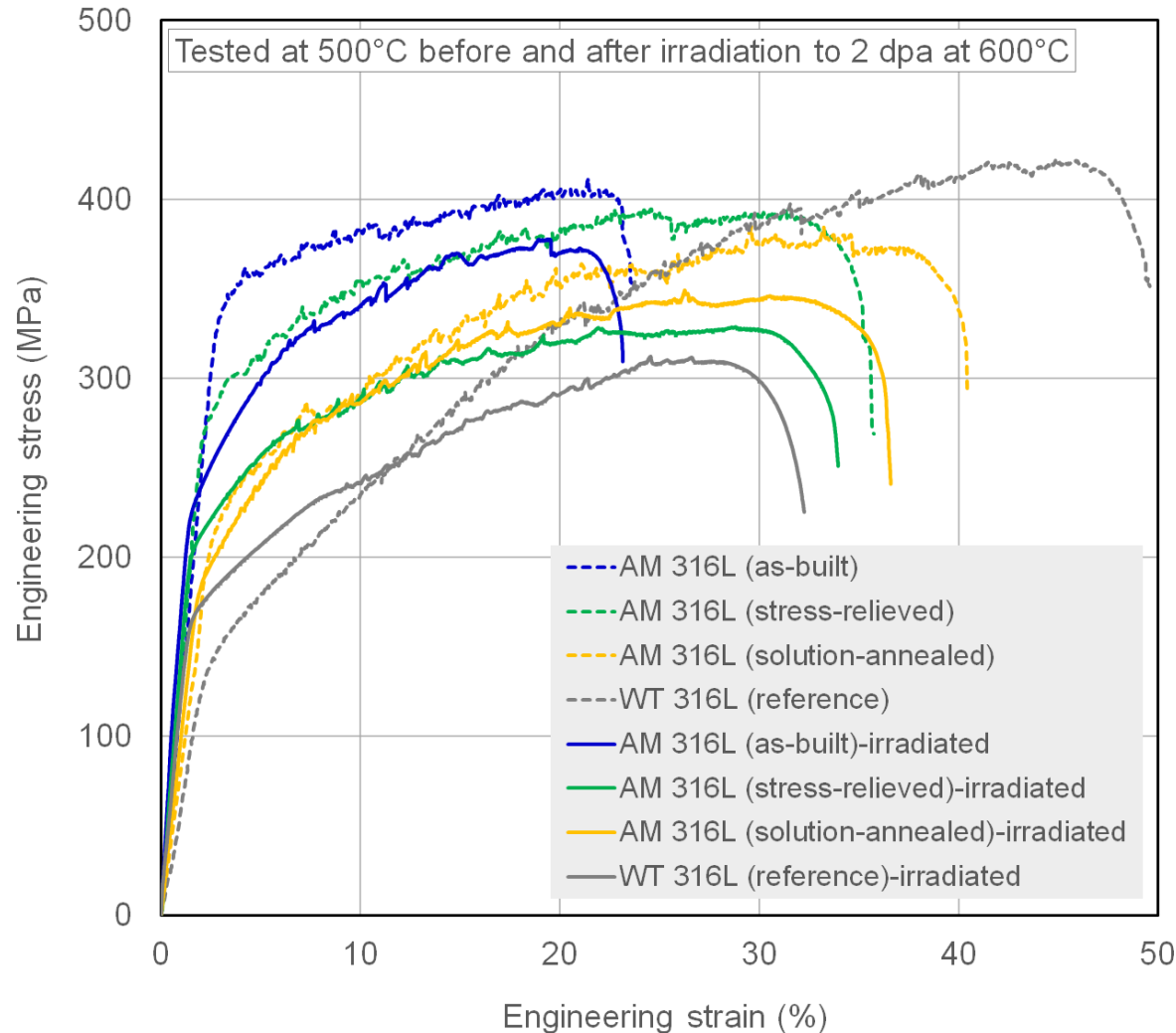
AM 316L and WT 316L after Irradiation: Tensile Curves at 300°C



Engineering stress-strain curves of AM 316L and WT 316L SSs tested at 300° C after irradiation to 2 dpa at 300° C.

➤ *A prompt necking at yield case is observed, but with significant necking ductility.*

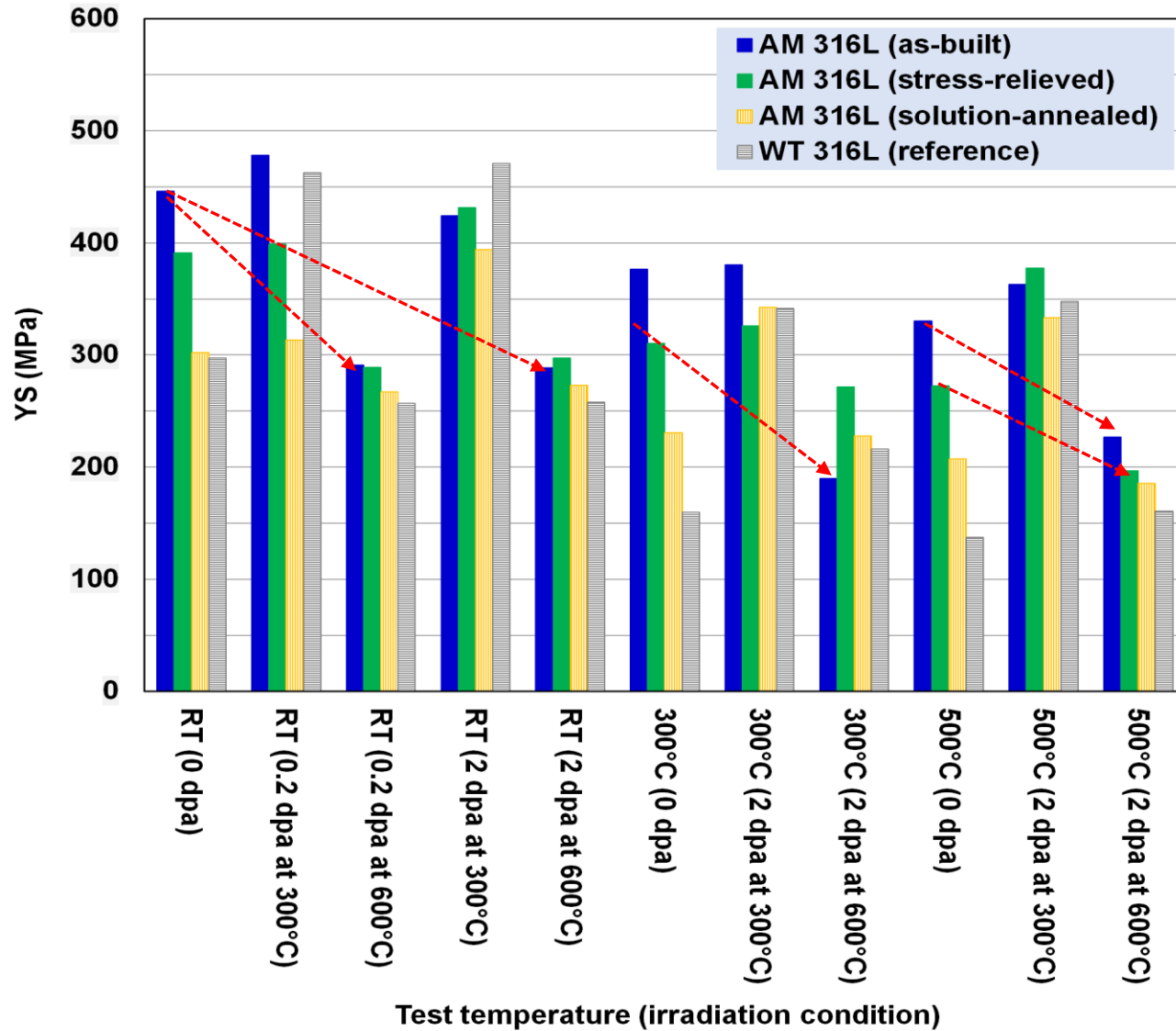
AM 316L and WT 316L after Irradiation: Tensile Curves at 500°C



Engineering stress-strain curves of AM 316L and WT 316L SSs tested at 500° C after irradiation to 2 dpa at 600° C.

- *Serrated flow occurs due to dynamic straining aging regardless of irradiation.*
- *Radiation effect is not significant except for the significant reduction of ductility in the reference material.*

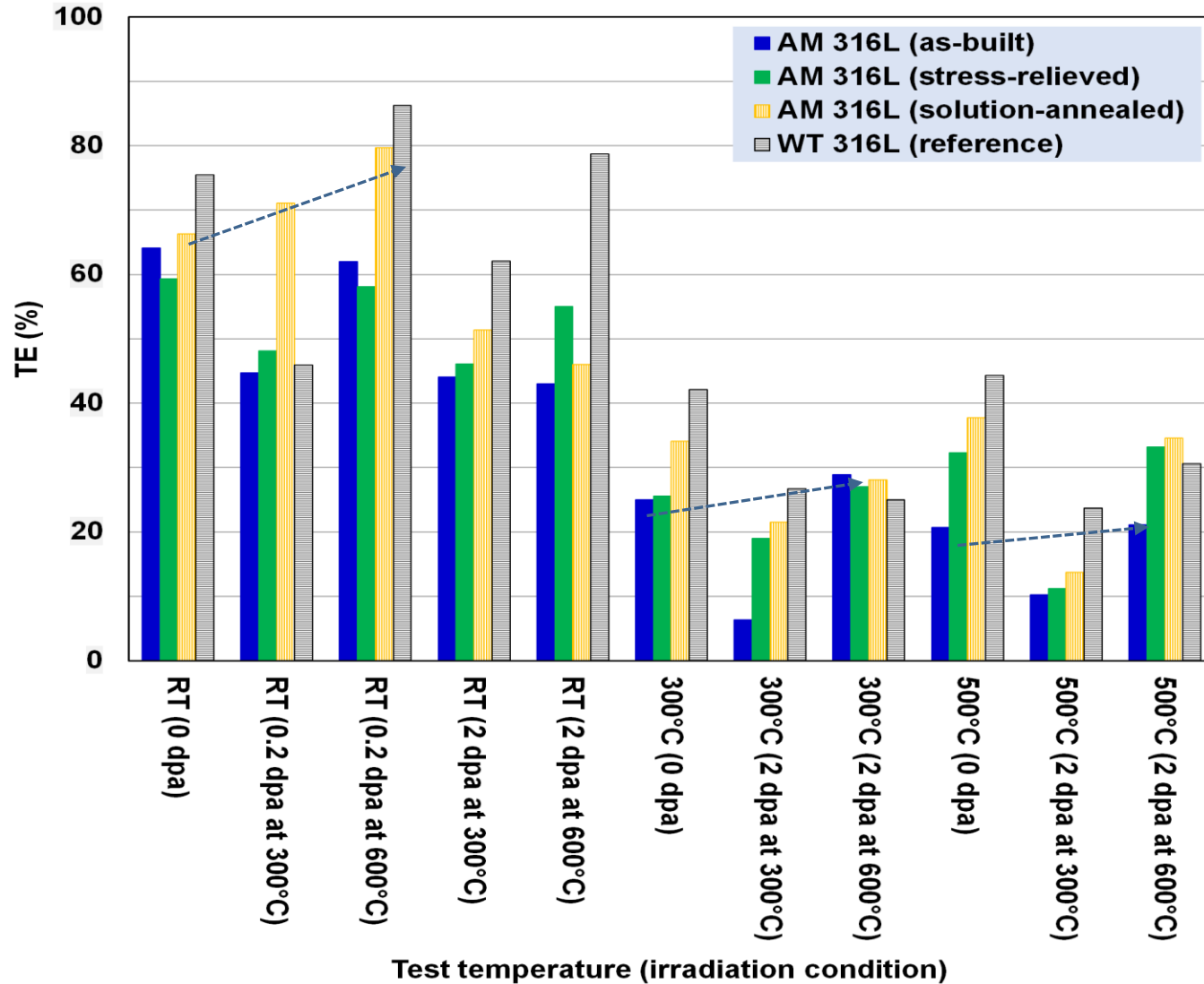
AM 316L and WT 316L after Irradiation: Strength



Comparison of tensile properties for AM and WT 316L SSs in various test and irradiation conditions: yield strength (YS).

- *Irradiation hardening is common for lower temperature (300 °C) irradiation.*
- *Irradiation softening is found at 500 °C) in the high strength (as-built, stress-relieved) microstructures after higher temperature irradiation.*

AM 316L and WT 316L after Irradiation: Ductility



Comparison of tensile properties for AM and WT 316L SSs in various test and irradiation conditions: total elongation (TE).

- *Ductility increase (ductilization) is found in many conditions after higher temperature (600 °C) irradiation.*

Summary

- 1) Neutron irradiation induces significant changes in the mechanical behavior of AM stainless steels, **including radiation-induced hardening and softening depending on irradiation temperature.**
- 2) **Irradiation hardening was lower in the stronger materials** (i.e., the as-built and stress-relieved AM SSs) than in the solution-annealed AM and WT SSs. Relatively low strength 316L SSs retained better ductility in general; however, the stronger 316L SSs demonstrated similar levels of ductility after the higher temperature (600 °C) irradiation.
- 3) The as-built 316L steel after 300°C irradiation showed unstable plastic deformation (i.e., necking) just after yielding, while the tensile behavior change was less significant after the higher temperature (600 °C) irradiation.
- 4) **Radiation-induced ductilization** was observed after the higher temperature irradiation. **No embrittlement** was observed within the tensile test or in the irradiation conditions explored. **This might be the key base for assessment of the AM 316L for in-reactor applications.**
- 5) **AM 316L SSs demonstrated limited radiation damage in properties as their unique microstructures, including high density grain boundaries and residual dislocations, can provide higher defect annihilation sites as well as necessary strength.**
- 6) **Going forward: Mechanical behavior after higher dose irradiation and effects of AM-induced defects on properties are to be evaluated.**

PERFORMANCE TESTING OF AM MATERIALS FOR STRUCTURAL APPLICATIONS IN NUCLEAR ENVIRONMENTS

BOGDAN ALEXANDREANU, XUAN ZHANG, YIREN CHEN, WEI-YING CHEN, AND MEIMEI LI

Nuclear Science and Engineering Division

Argonne National Laboratory

AMMT Program Review Meeting, May 18 – 19, 2022

RESEARCH ACTIVITIES AT ANL

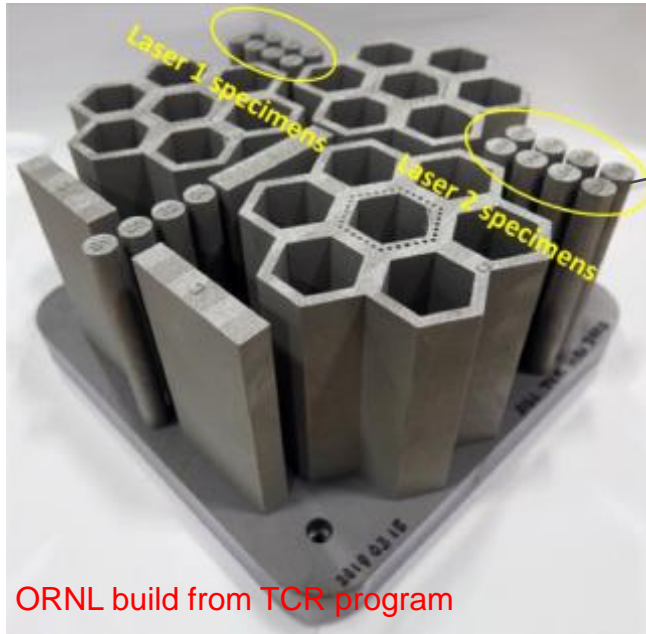
- **Creep properties of AM 316L (ORNL build)**
 - Comparison of as-built AM with conventionally-produced alloys
 - Effect of heat treatment
 - Effect of location (and sub-sized vs. standard specimens)
- **Fatigue and creep-fatigue properties of AM 316L (ORNL build)**
 - Effect of temperature (300°C and 550°C)
 - Creep-fatigue at 550°C
- **SCC and corrosion-fatigue crack growth response of AM316L (ANL build)**
 - Performance testing conducted in LWR environment
- **Development of AM 316H (ANL build)**
 - Microstructure
 - Tensile testing at RT and 550°C

CREEP

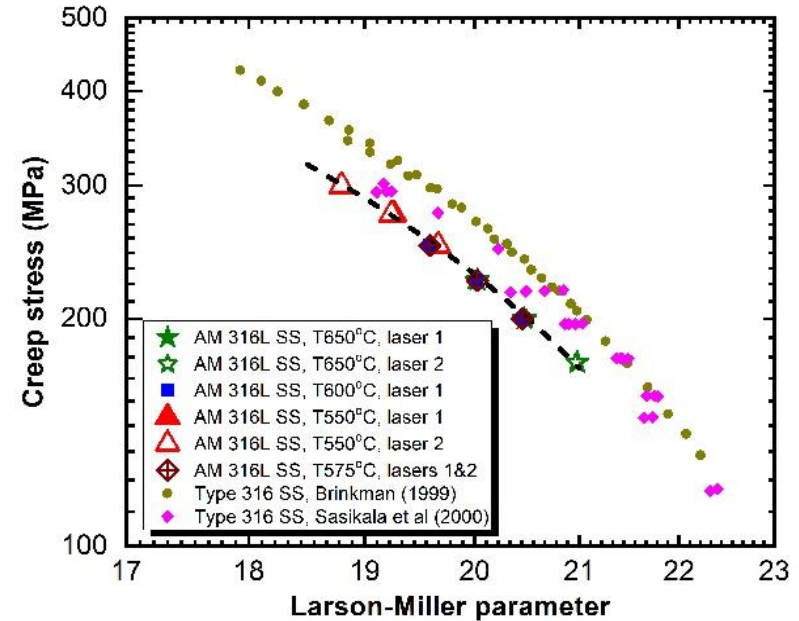
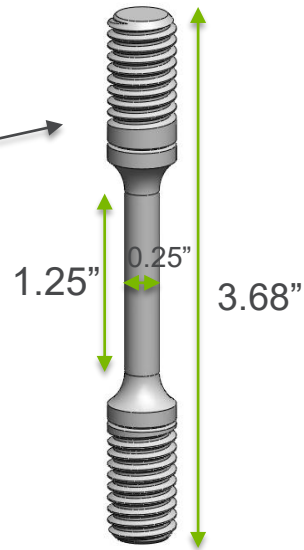


CREEP TESTING OF AS-BUILT AM 316L

Comparison with conventionally-produced alloys



ORNL build from TCR program

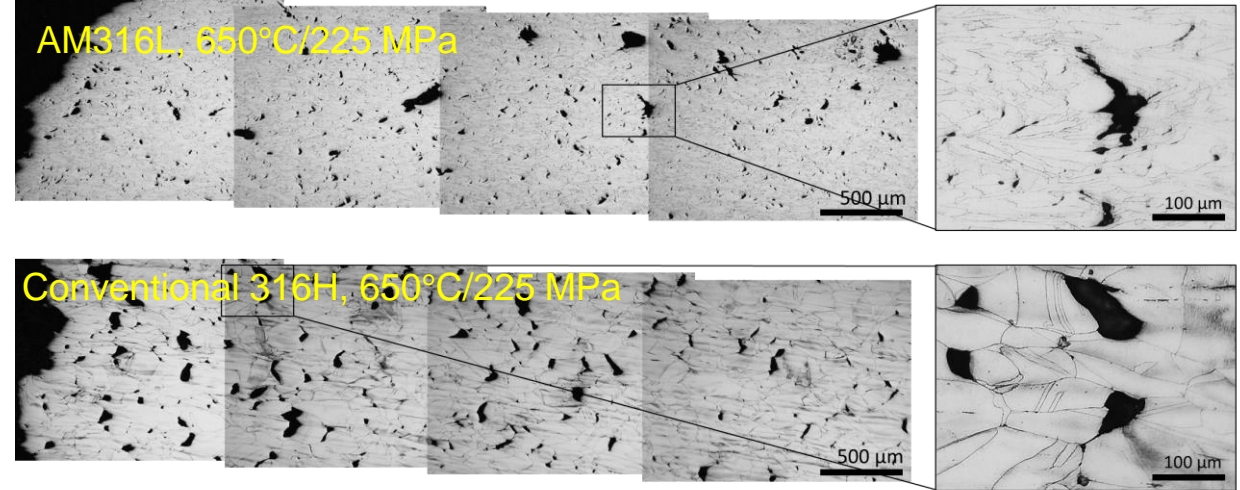
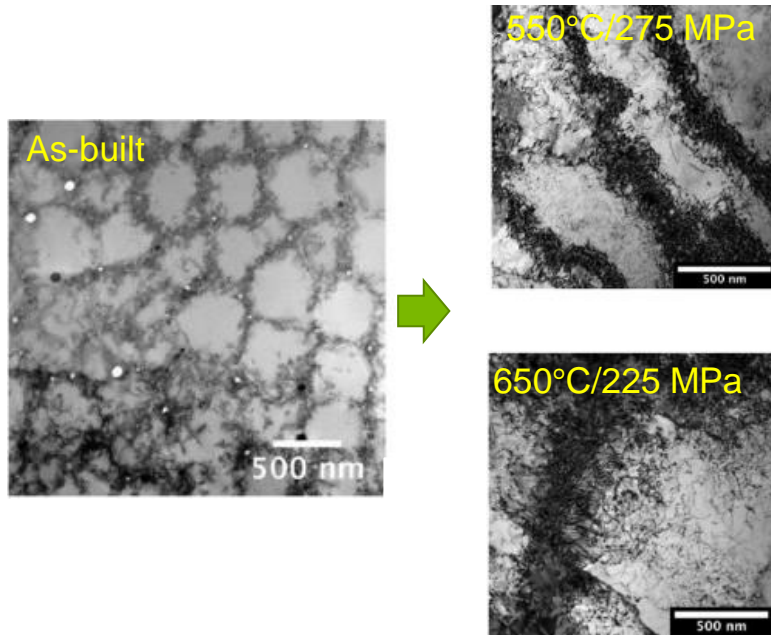


Li, M., Zhang, X., Chen, W. Y., & Byun, T. S. (2021). *Journal of Nuclear Materials*, 548

- Creep testing was conducted on ASTM standard-sized specimens from rods at 550°C, 575°C, 600°C and 650°C
- The creep data of all the specimens (conventional and AM, either laser) can be described by a single Larson-Miller plot
- Relative to conventional 316 SS, as-built AM 316L SS has an inferior creep rupture strength

CREEP TESTING OF AM 316L

AM microstructure effects on creep



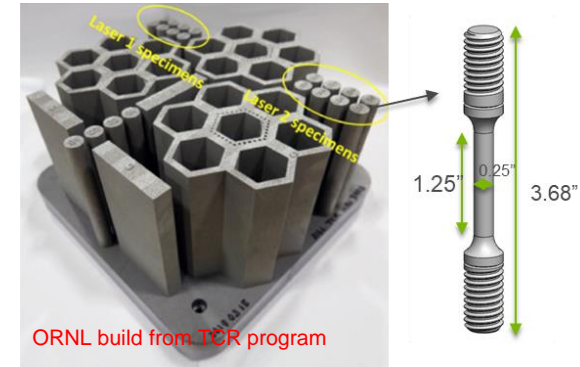
Li, M., Zhang, X., Chen, W. Y., & Byun, T. S. (2021). *Journal of Nuclear Materials*, 548.

- Secondary creep: The dislocation cell structure formed during printing limits the work hardening capability, and it is not stable under creep, thus shortening the steady-state creep stage

- Tertiary creep: Both AM and conventional material failed by intergranular cracking in tests
- AM material has a higher density of smaller cracks (+ low density of large cracks) compared to the conventional material (large density of large cracks)
- The reduced creep life of the AM material may be due to a shortened void nucleation stage (built-in voids precursors were already in place)

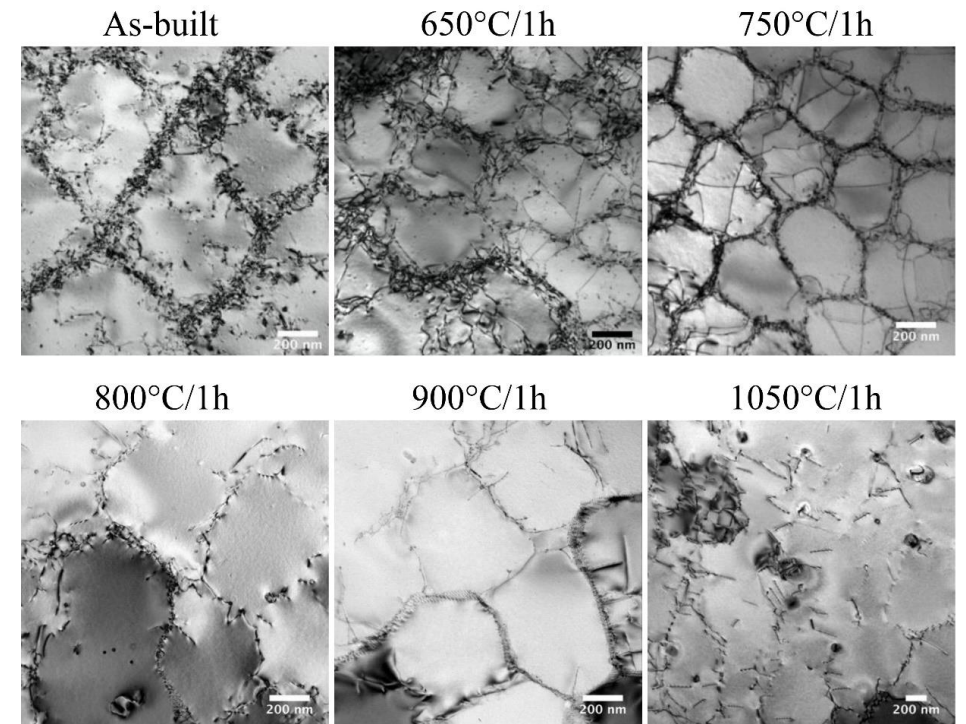
CREEP TESTING OF AM316L

Heat treatment effect



List of heat treated rod specimens and creep testing conditions

Specimen ID	Build ID	Rod ID	Laser mode	HT Condition	Test Temp (°C)	Stress (MPa)
L106	20190308M2	L1	Laser 1	650°C/1h	550	275
L206	20190308M2	L2	Laser 2	650°C/1h	550	275
S-4	20190315M2	S-4	Laser 1&2	700°C/1h	550	275
L2-3	20190315M2	L2-3	Laser 2	750°C/1h	550	275
L2-4	20190315M2	L2-4	Laser 2	800°C/1h	550	275
L1-4	20190315M2	L1-4	Laser 1	900°C/1h	550	275
L205	20190308M2	L2	Laser 2	1050°C/1h	550	275

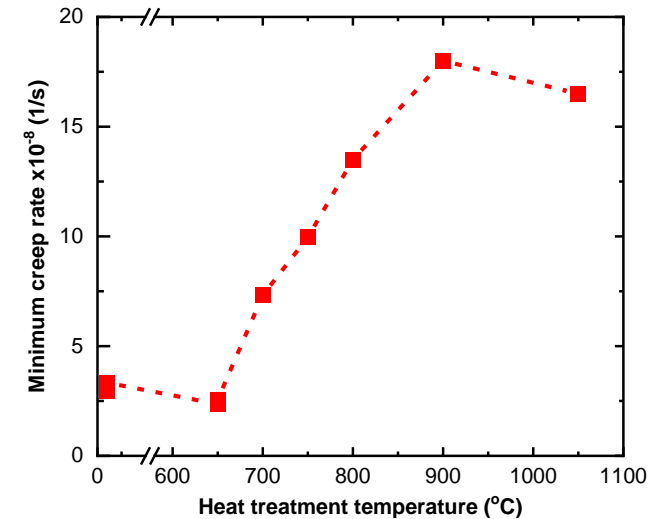
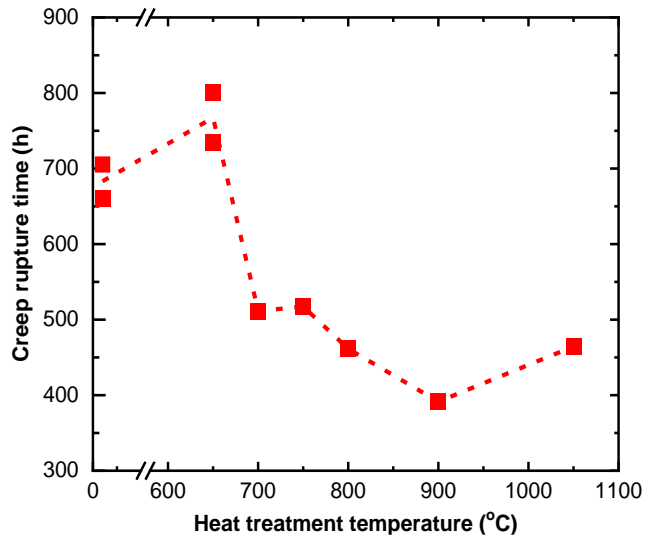
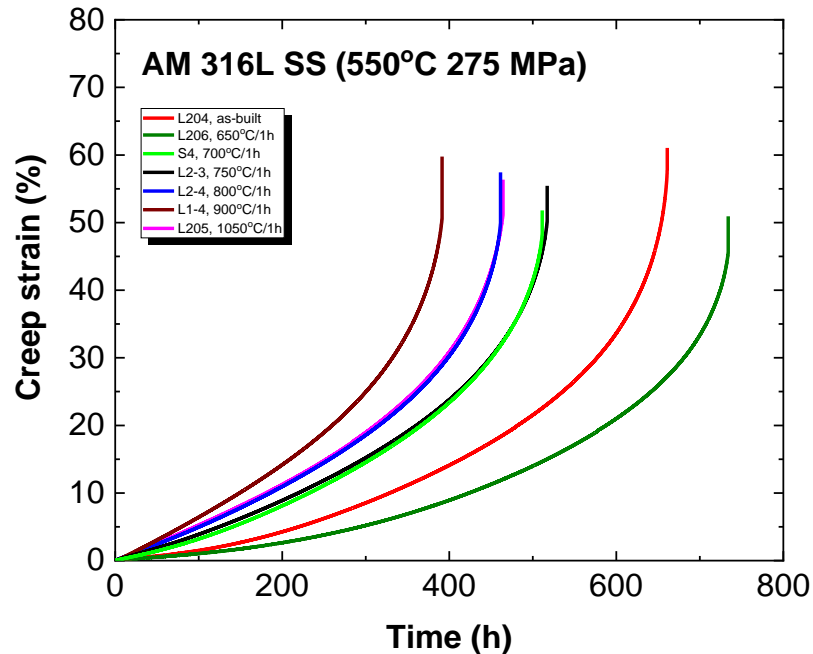


Li, M., Chen, W. Y., Zhang, X., (2022). *Journal of Nuclear Materials*, 559

- Heat treatments ranged from typical stress relief to solution annealing (SA, 1050° C)
- The SA heat treatment removed the dislocation cell structures

CREEP TESTING OF AM316L

Heat treatment effect

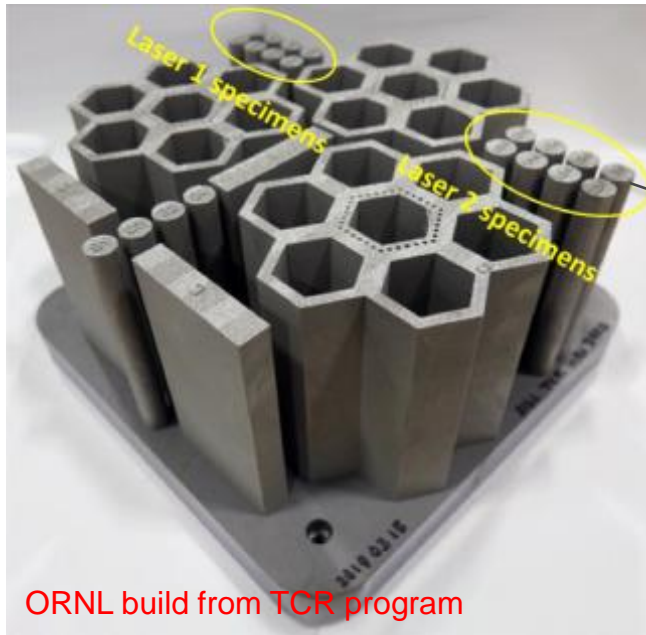


Li, M., Chen, W. Y., Zhang, X., (2022). *Journal of Nuclear Materials*, 559, 153469.

- The creep life shows a maximum with 650°C treatment
- The minimum/secondary creep rate shows a minimum with 650°C treatment

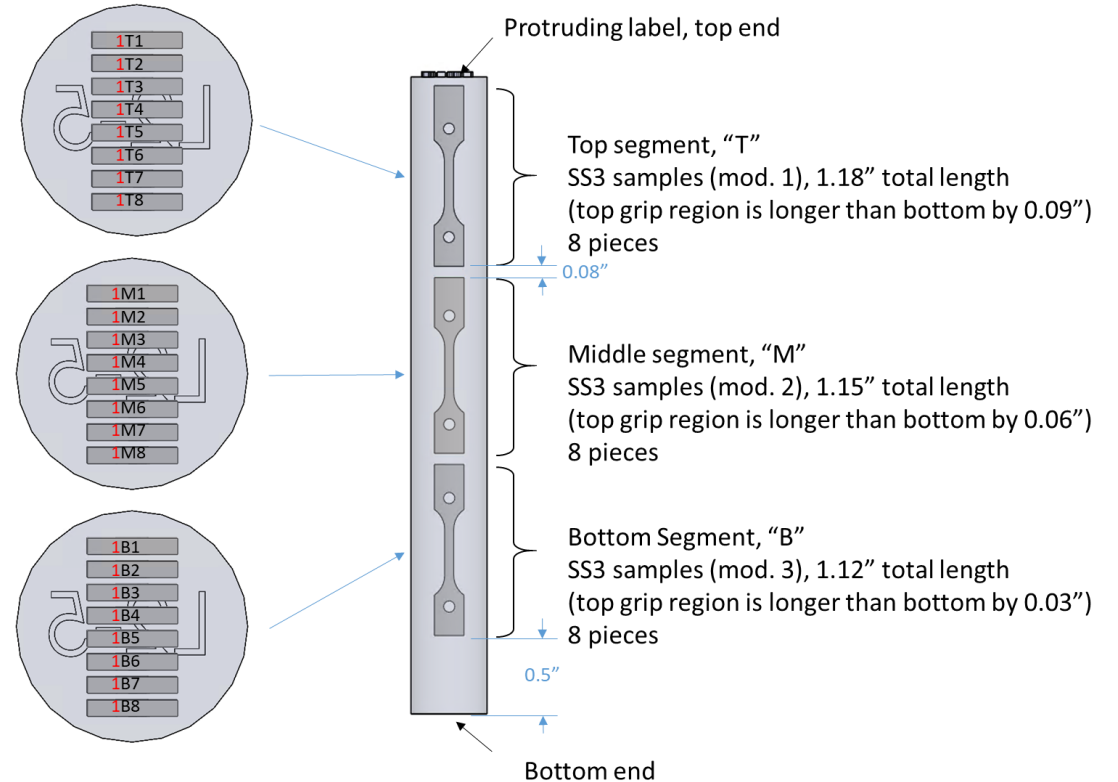
CREEP TESTING OF AM316L

Location-specific testing (on-going)



Example:

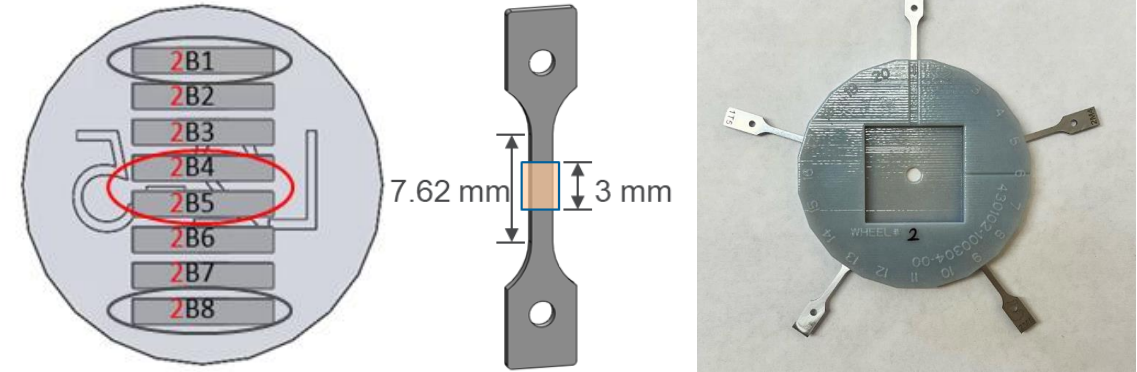
Rod ID L1-8



- Location-dependent microstructure/porosity is expected to affect creep response
- Creep tests on SS-3 type creep specimens extracted from different locations were performed at 550°C

POROSITY MEASUREMENT WITH X-RAY TOMOGRAPHY

High-throughput data acquisition and analysis

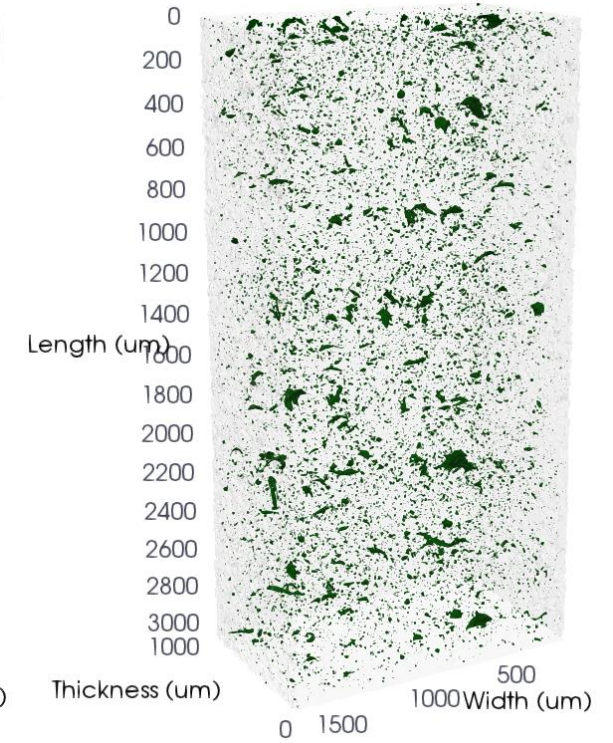
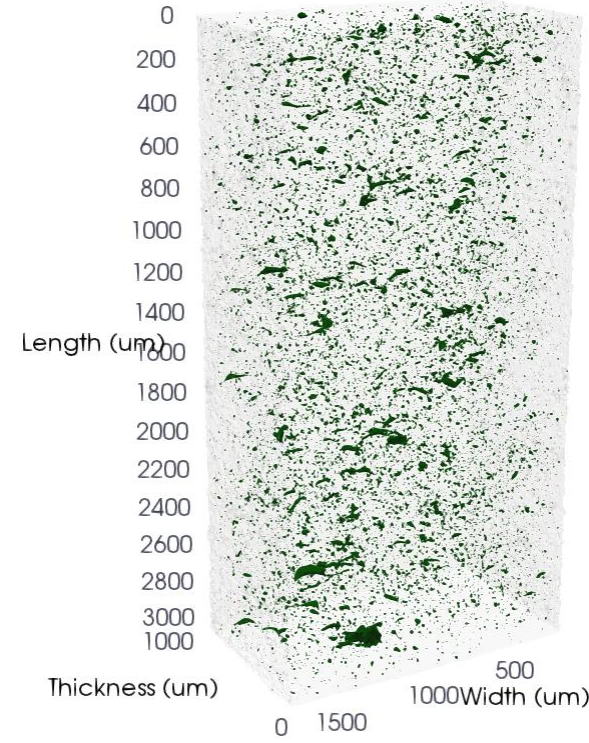
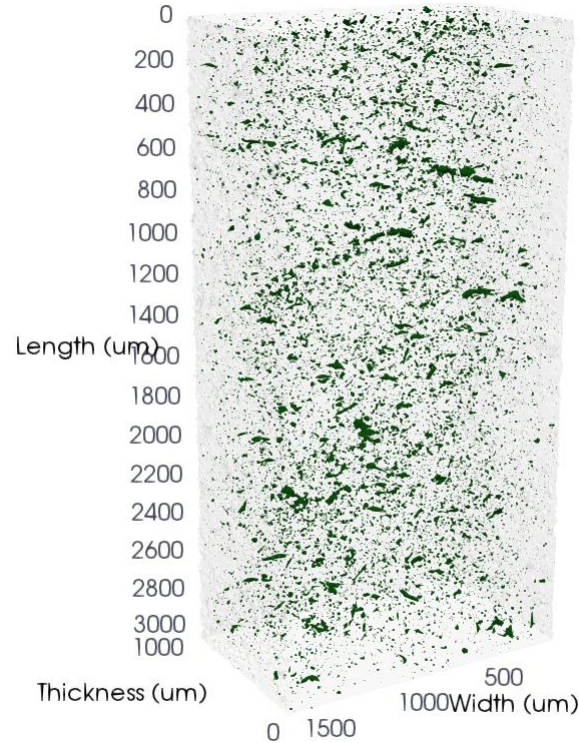
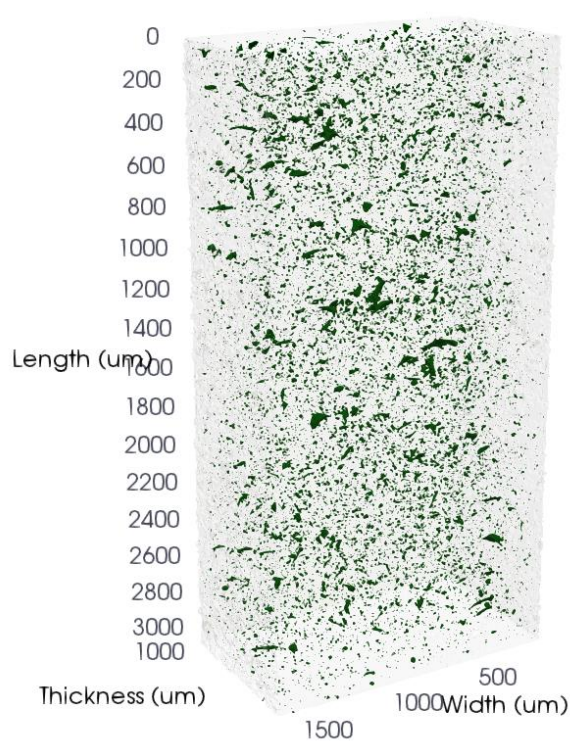


2B1, Porosity: 0.21%

2B4, Porosity: 0.18%

1B5, Porosity: 0.19%

1B8, Porosity: 0.21%



2B1	Mean	Median	Std. Dev.
Volume (μm^3)	371.336	128.787	2027.374
Max. Feret Diameter (μm)	11.698	10.082	8.283
Eq. Vol. Diameter (μm)	7.138	6.266	3.121
Ellipticity (Equ.)	0.35	0.349	0.160
Ellipticity (Polar)	0.501	0.508	0.139

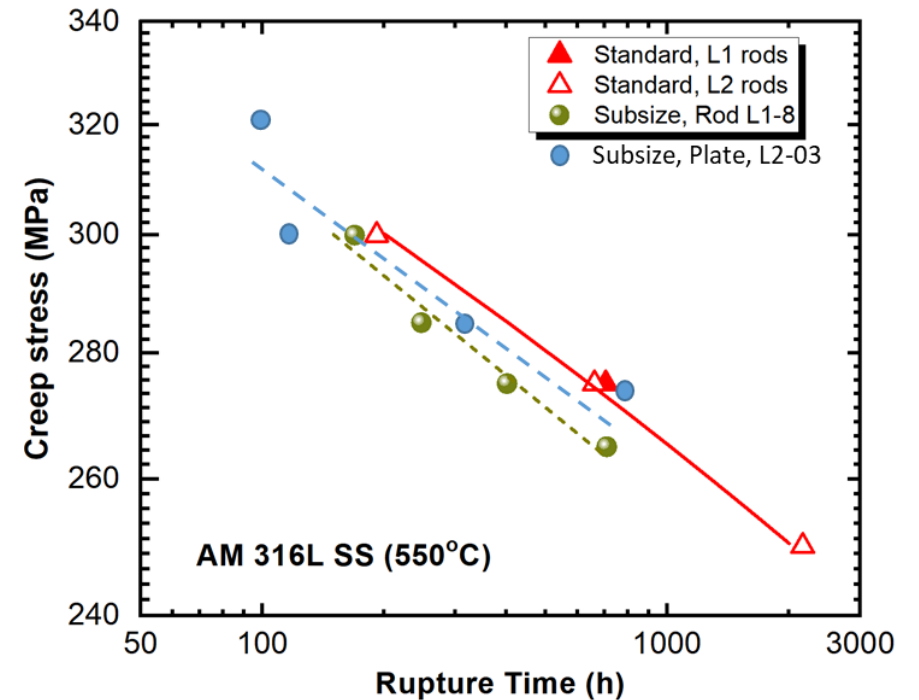
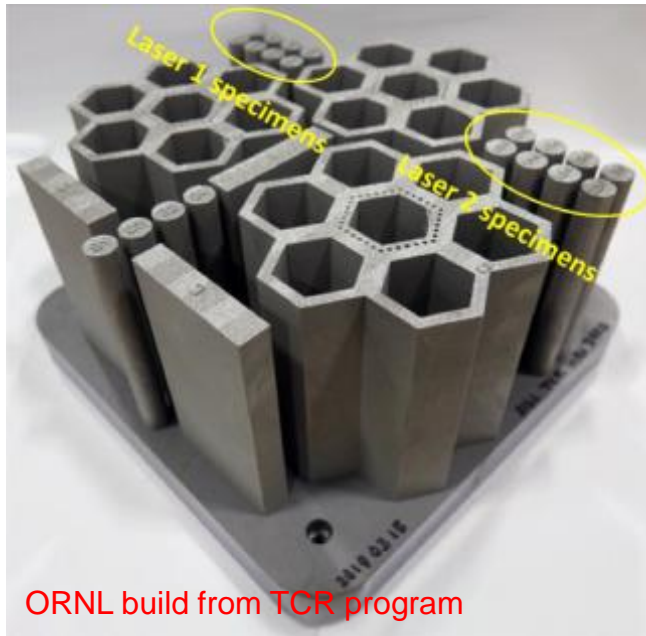
2B4	Mean	Median	Std. Dev.
Volume (μm^3)	340.184	128.787	1601.207
Max. Feret Diameter (μm)	11.718	10.082	8.579
Eq. Vol. Diameter (μm)	7.079	6.266	2.963
Ellipticity (Equ.)	0.355	0.355	0.162
Ellipticity (Polar)	0.505	0.512	0.142

1B5	Mean	Median	Std. Dev.
Volume (μm^3)	353.074	125.568	3354.28
Max. Feret Diameter (μm)	11.719	10.082	8.498
Eq. Vol. Diameter (μm)	7.026	6.213	2.993
Ellipticity (Equ.)	0.360	0.360	0.165
Ellipticity (Polar)	0.508	0.512	0.144

1B8	Mean	Median	Std. Dev.
Volume (μm^3)	400.977	130.397	3818.733
Max. Feret Diameter (μm)	11.841	10.082	8.452
Eq. Vol. Diameter (μm)	7.115	6.292	3.172
Ellipticity (Equ.)	0.374	0.378	0.164
Ellipticity (Polar)	0.519	0.526	0.140

CREEP TESTING OF AM 316L

Location-specific testing (on-going)



- Testing – involving specimens from both rods and plates - is on-going
- Preliminary data suggests that the use of sub-sized specimens has a minimal effect on data

FATIGUE AND CREEP-FATIGUE

FATIGUE AND CREEP-FATIGUE TESTING

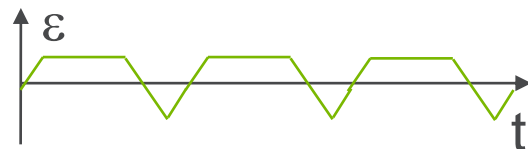
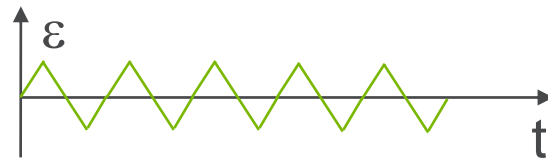
OBJECTIVES

- Evaluate the effects of internal defects and microstructure on fatigue and creep-fatigue properties of AM materials
- Evaluate the effects of print geometry and orientation on fatigue properties
- Generate baseline fatigue and creep-fatigue data to support ASME Code fatigue design rules

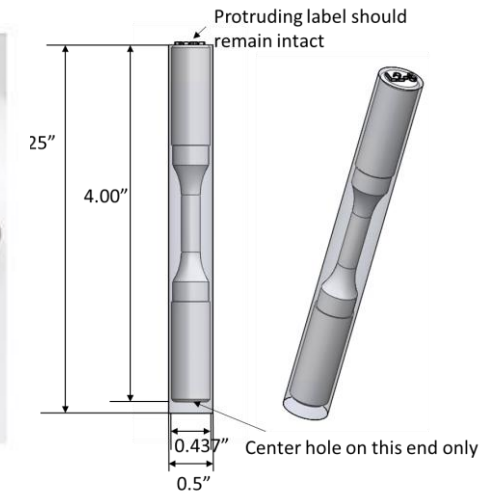
TESTING CAPABILITIES



Two servo-hydraulic systems capable of **strain-controlled** fatigue, creep-fatigue testing up to 1000° C in air atmosphere

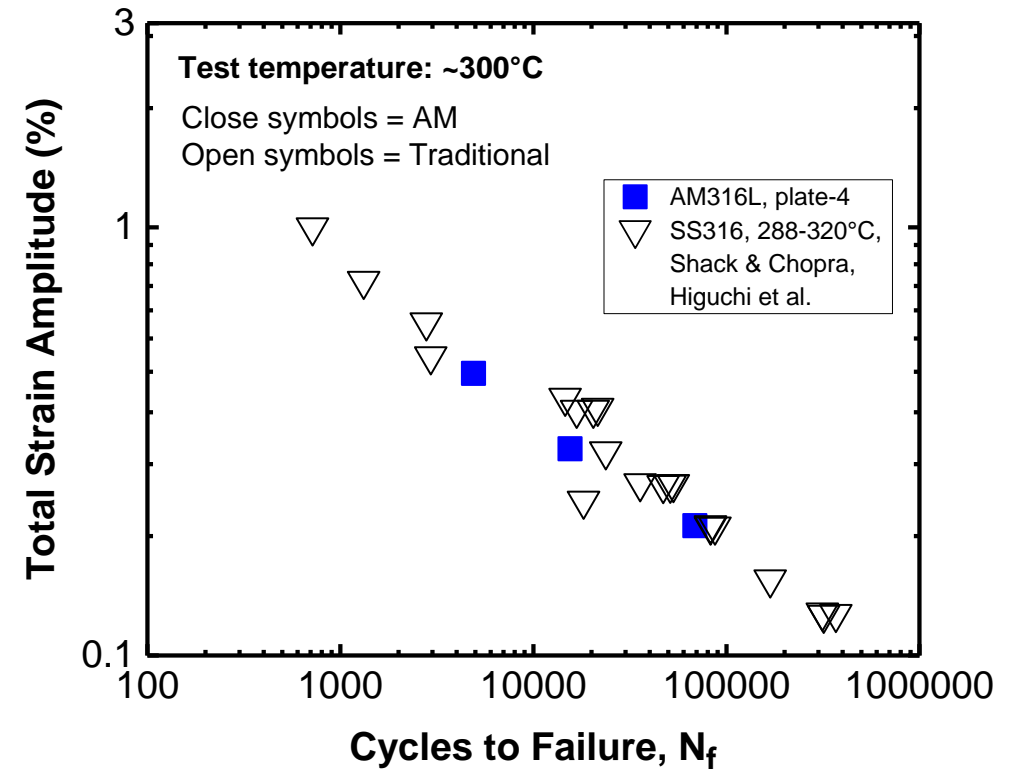
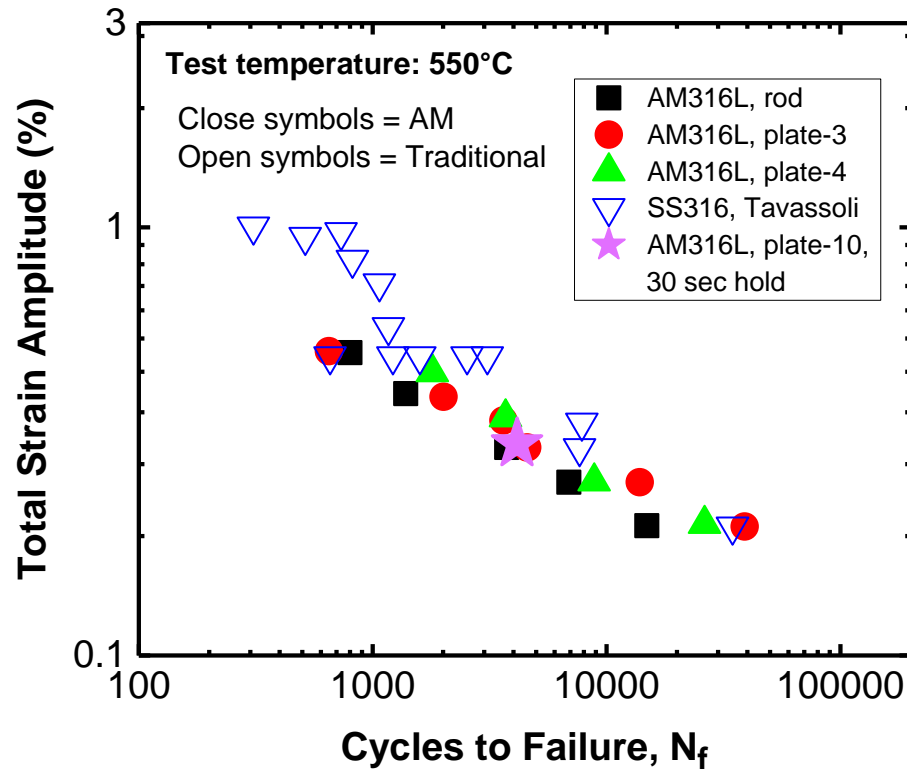


Specimens machined from **rods** of ORNL Build 20190315M2.



Specimens machined from **plates** of ORNL Build 20201009M2 in two build orientations: Horizontal vs vertical.

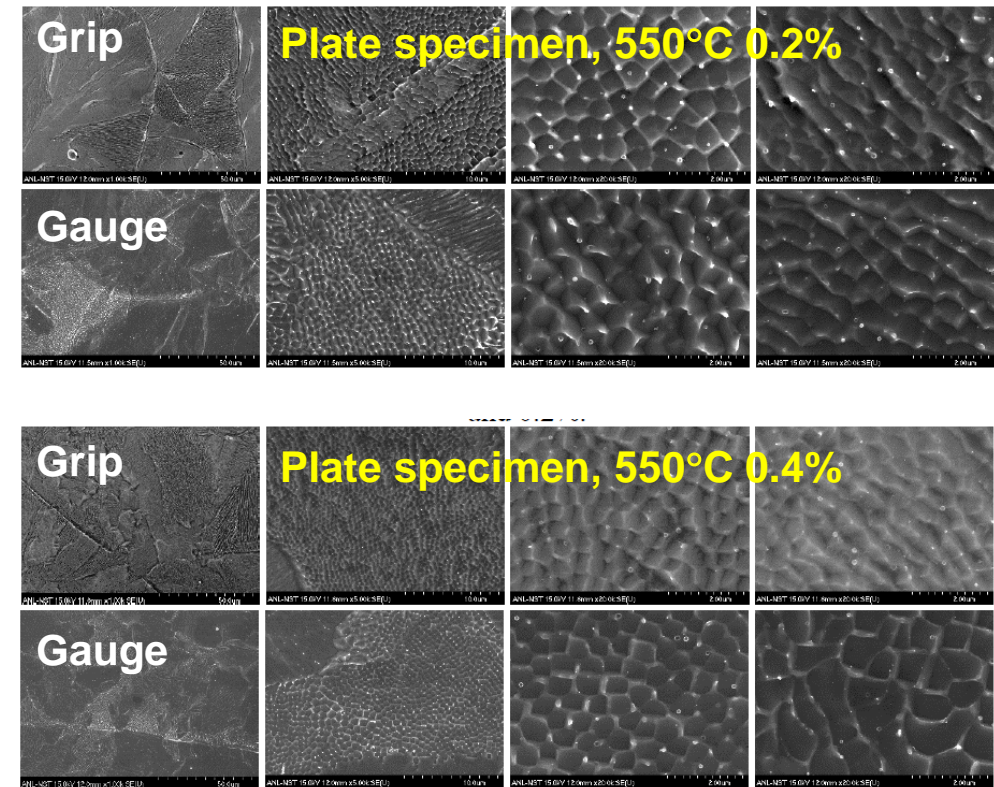
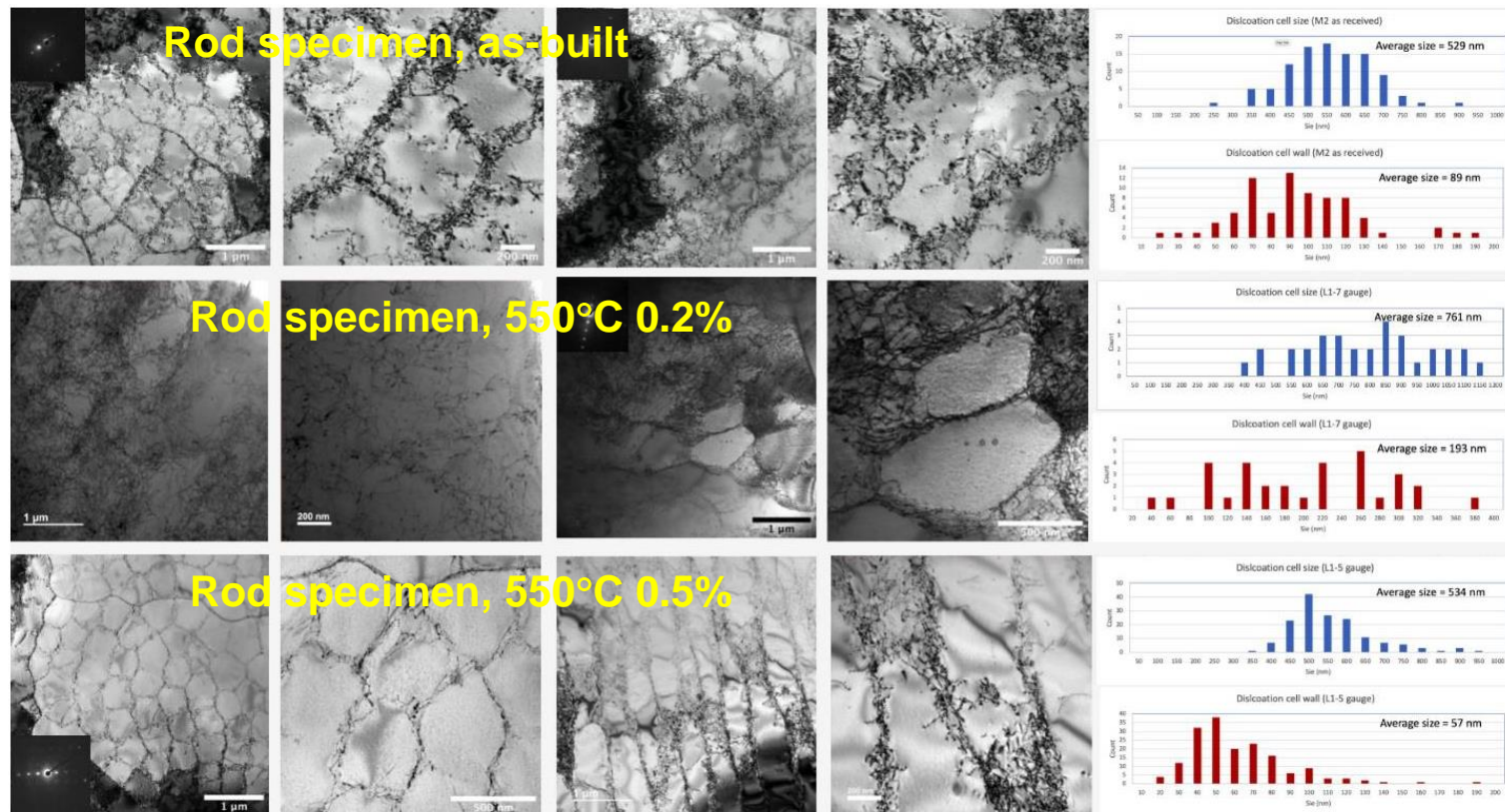
STRAIN-LIFE DATA OBTAINED TO DATE



- At **550° C**, AM316L may perform slightly worse than conventional 316L at high strain amplitudes
- The effect of print geometry, orientation, and location is insignificant
- **Short hold-time of 30 sec in tension does not show any detrimental effect**

- At **300° C**, creep lives are longer
- AM316L is similar to conventional 316L
- More data are needed at high strain amplitudes

MICROSTRUCTURAL EVOLUTION UNDER FATIGUE



- Qualitatively insignificant changes in cell structures under fatigue loading in AM 316L SS

CRACK GROWTH RATE TESTING IN LWR ENVIRONMENT

OBJECTIVES AND APPROACH

Background

- EPRI-led ASME Code Case for pressure boundary applications
- Qualification and regulatory acceptance of AM components is expected to involve a performance-based approach

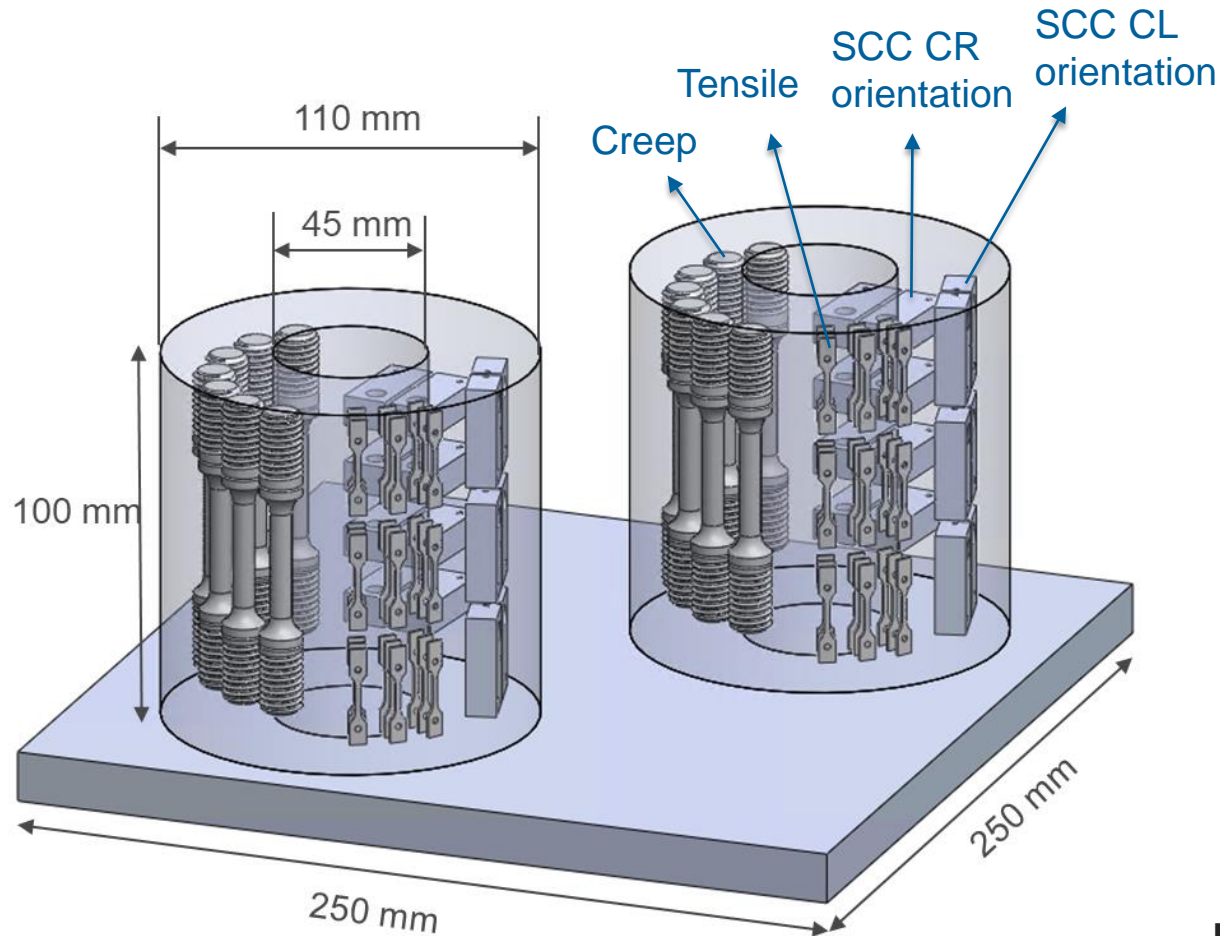
Objective

- Evaluate the “performance” of AM 316L SS in a light water reactor (LWR) environment

Approach

- Build a component-like part using laser powder bed fusion (LPBF)
- Conduct microstructural investigation (with a focus on porosity)
- Conduct mechanical testing with a focus on “performance testing” - crack growth by corrosion fatigue and stress corrosion cracking (SCC) in a LWR environment, and compare with the behavior of the conventionally-produced alloys

AM 316L SS PERFORMANCE TESTING



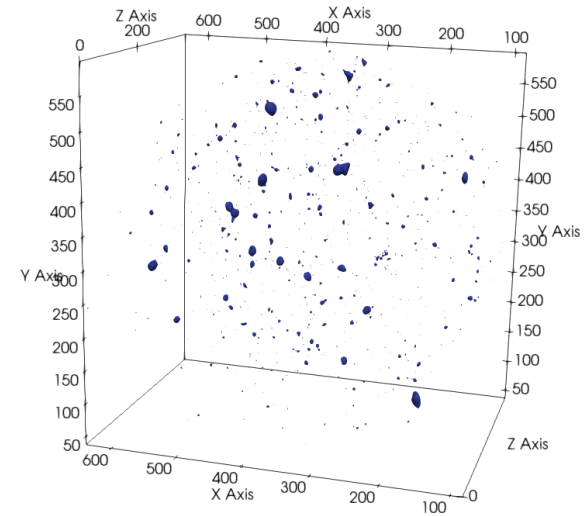
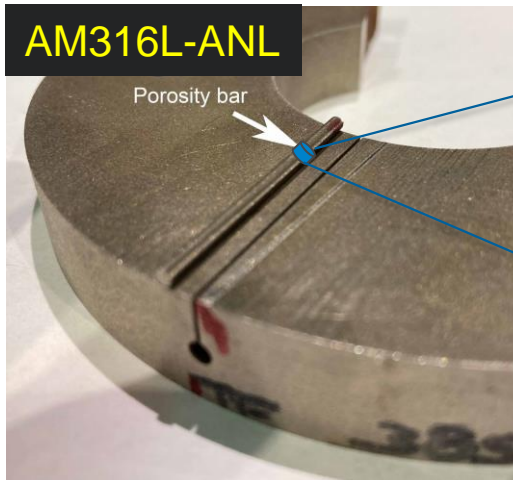
Environmentally-assisted Cracking Laboratory at ANL



- AM 316L SS tubes were produced at Argonne with the Renishaw AM400 LPBF system

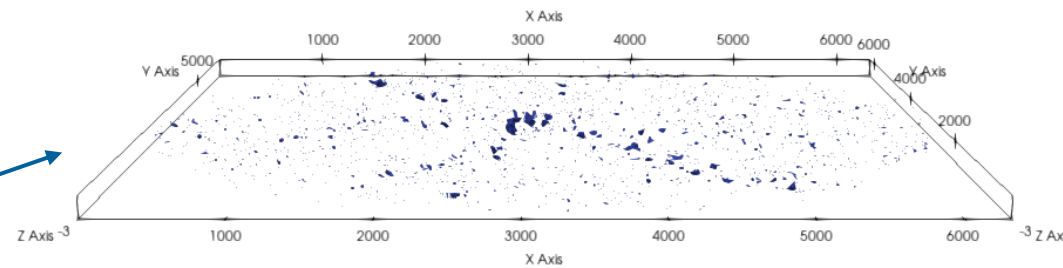
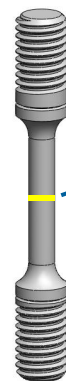
- Crack growth rate (CGR) testing was conducted using one of the several dedicated systems at ANL in simulated LWR environment

POROSITY MEASUREMENTS



- Volumetric porosity measured by synchrotron X-ray CT: **0.06%**

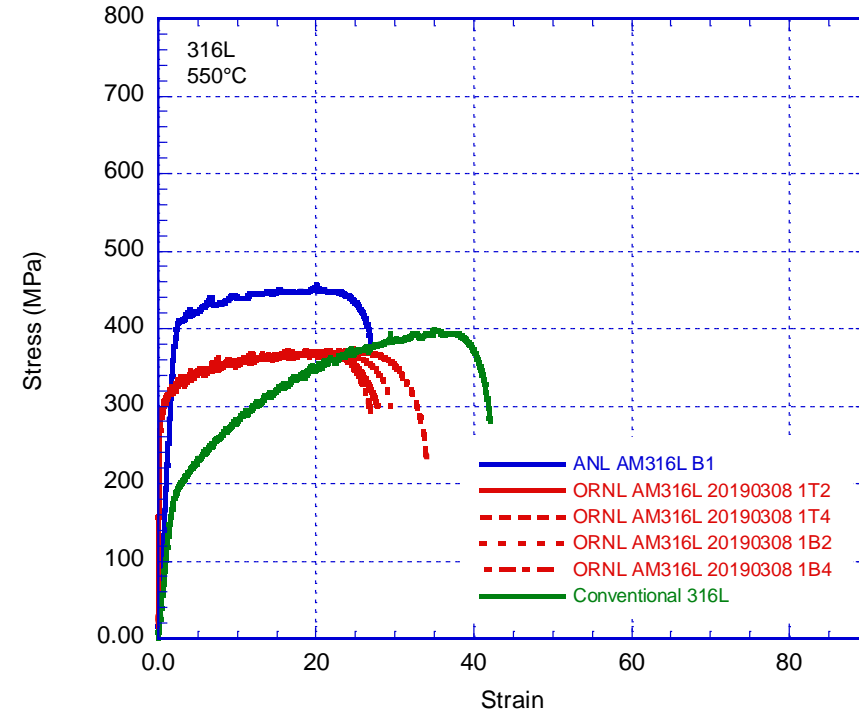
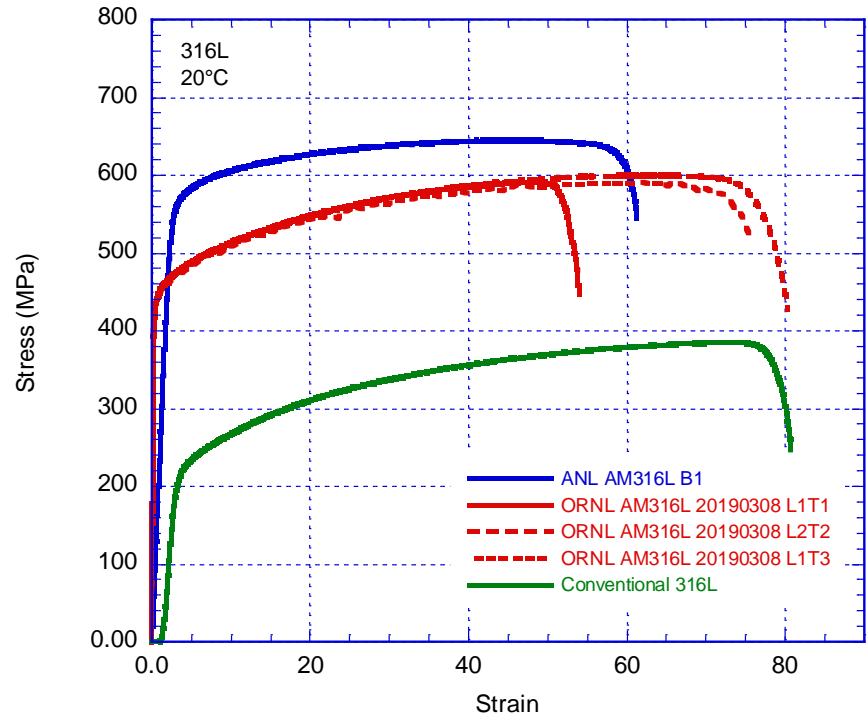
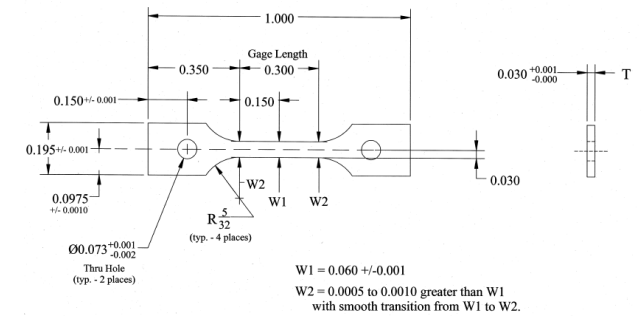
AM316L-ORNL



- Volumetric porosity measured by synchrotron X-ray CT: **0.10%**

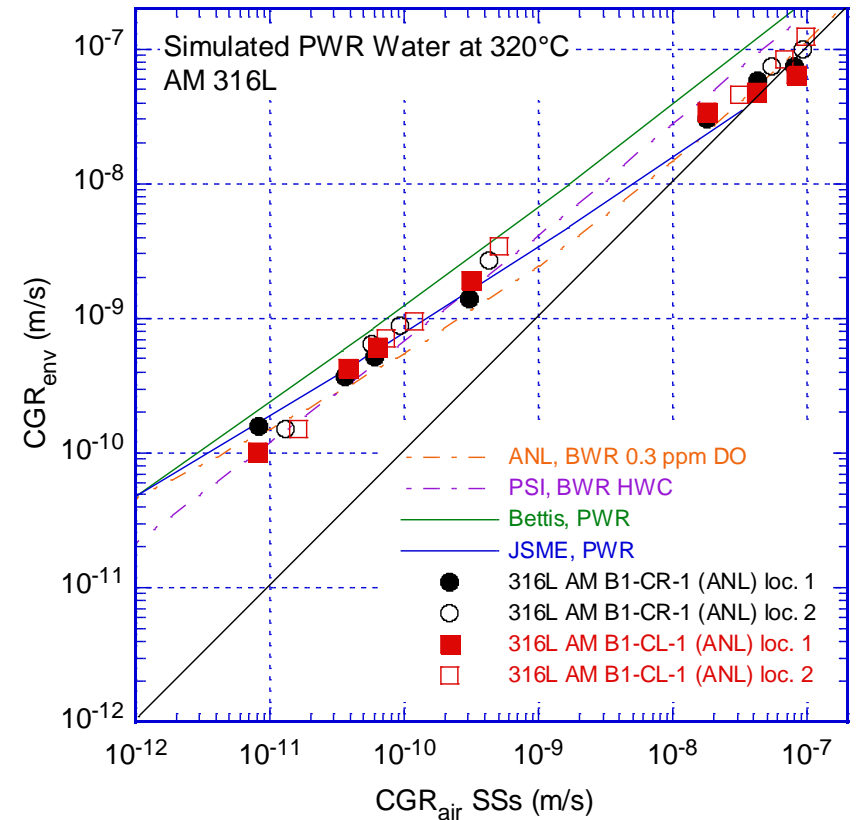
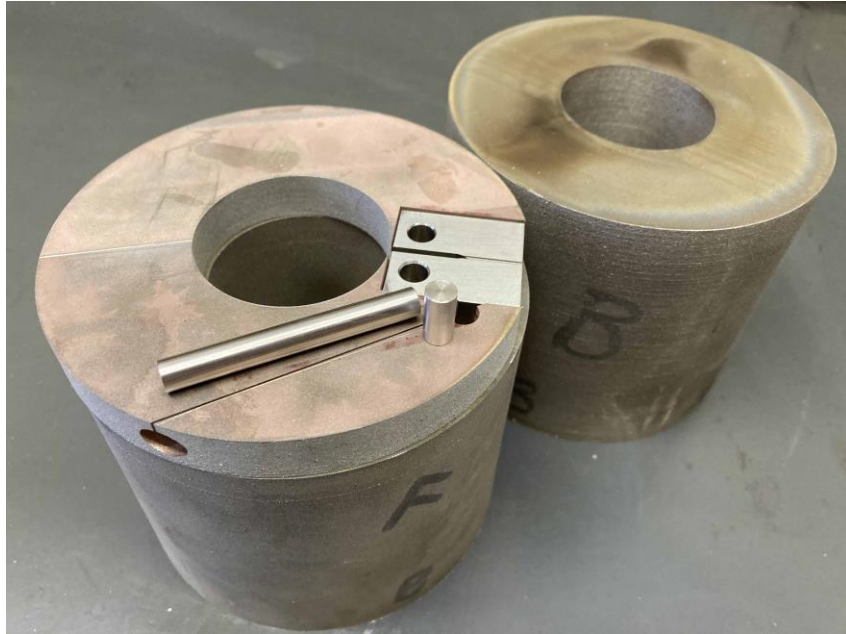
TENSILE TESTING

- SS-3 type specimens



- At RT and 550°C, tensile properties of ANL AM 316L build are comparable to those of ORNL AM 316L plate and those of the conventional alloy
- ANL and ORNL use different 3D printers

CYCLIC AND SCC CGR RESPONSE OF AM 316L



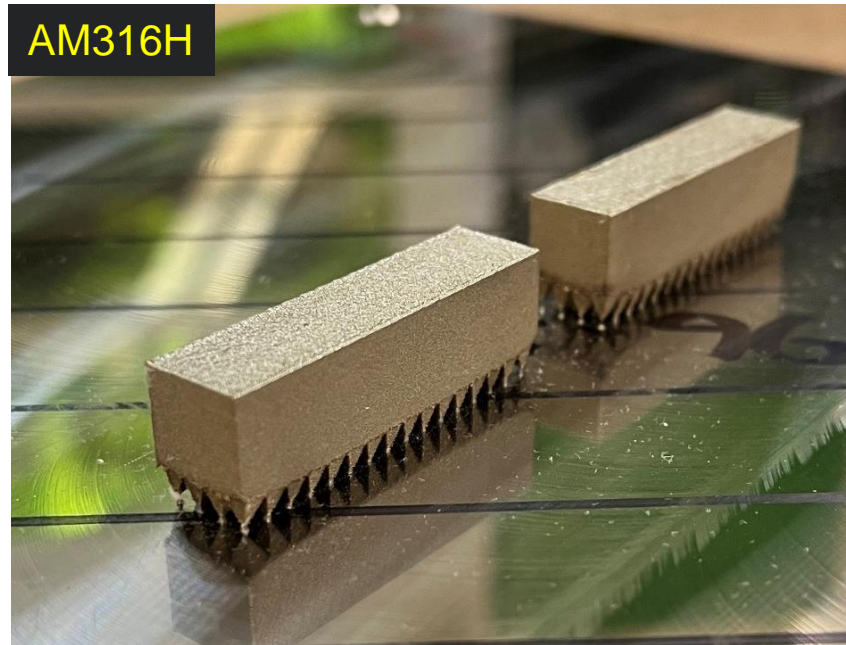
- Fatigue and corrosion fatigue CGR response (2 locations along the crack path) is similar to that of conventionally-produced alloy
- AM 316L was resistant to SCC (2 attempts at 2 locations)

ALLOY 316H

ANL BUILD OF 316H



Parameter	Value
Laser Power	195 W
Layer Thickness	50 μm
Rotation	67 degrees
Exposure Time	80 μs
Point Distance	60 μm
Effective Velocity	0.75 m/s
Hatch Spacing	110 μm
Build Chamber Atmosphere	Argon



Sample ID:	316L-B1	4M316H-
Solids	WT %	WT%
Oxygen	.037	.046
Nitrogen	.095	.015
Carbon	.017	.040
Sulfur	.009	.005
Iron	67.29	66.46
Chromium	16.55	17.04
Manganese	.57	1.09
Silicon	.59	.45
Nickel	12.33	12.22
Copper	.12	.007
Molybdenum	2.26	2.57
Vanadium	.057	.010
Phosphorus	.013	.018
Cobalt	.058	.028
Tungsten	<.002	<.002

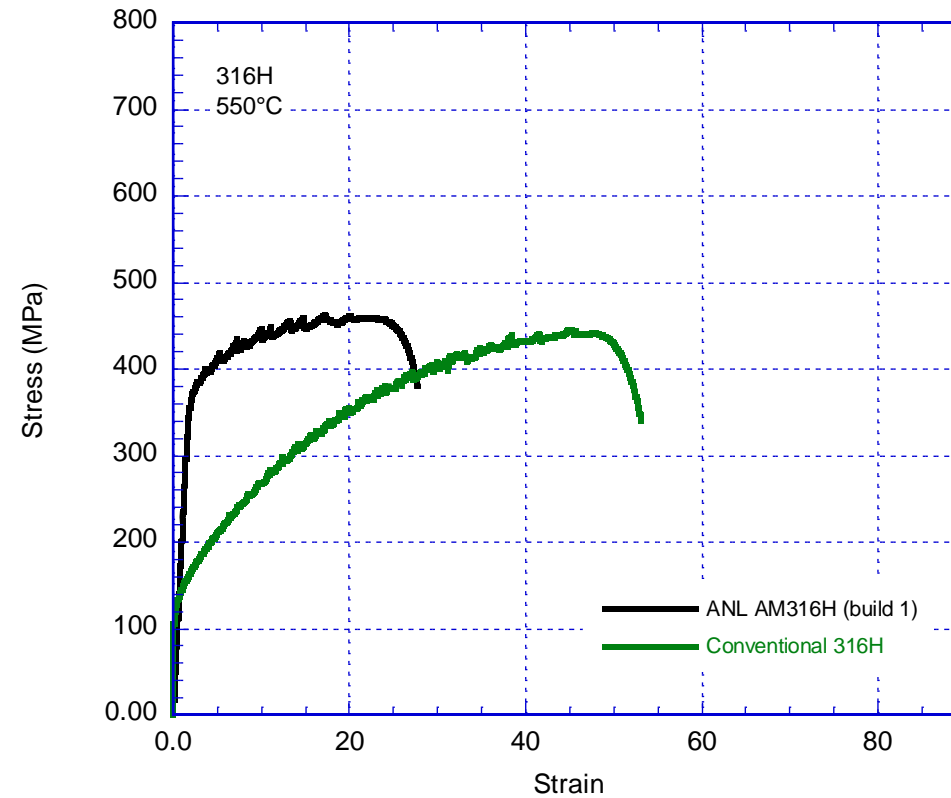
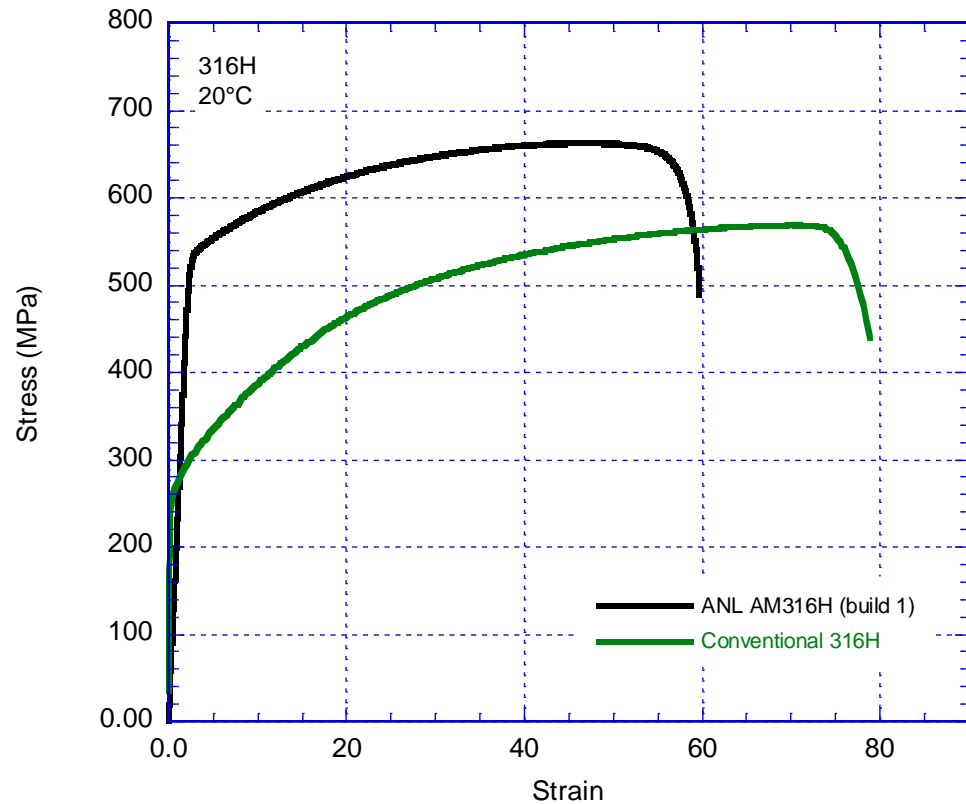
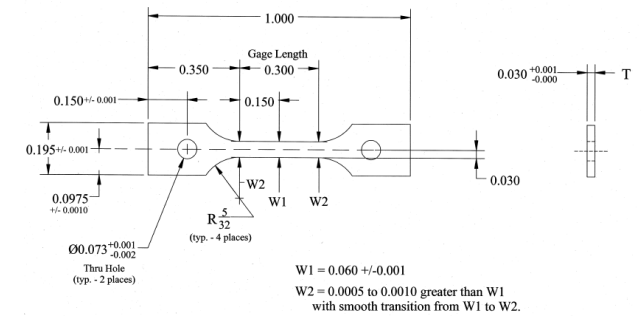
- AM 316H was produced at Argonne with the Renishaw AM400 LPBF system with the same parameters that were used for the 316L build



Areal porosity: **0.21%**

TENSILE PROPERTIES

- SS-3 type specimens



- Tensile properties of ANL AM 316H vs. conventional 316H at RT and 550°C

SUMMARY

- Effects of location/anisotropy in AM 316L on tensile properties, creep, fatigue and creep-fatigue are under investigation
- Creep rupture of as-built AM 316L appears to be inferior to that of conventional alloy
- Fatigue behavior of AM 316L alloy appears to be similar to those of conventional alloys, and a 30-sec hold time does not show any detrimental effect
- For performance evaluation in LWR environment, two component-like tubes of AM 316L were produced at ANL, porosity was found to be small (0.06%)
- Crack growth rate testing in LWR environment revealed that fatigue, corrosion fatigue, and SCC CGR response of AM alloy in the “as-built” condition is similar to that of the conventionally-produced alloy
- AM 316H was produced at ANL, and initial evaluations are in progress

ACKNOWLEDGEMENTS

- The authors gratefully acknowledge financial support from US DOE Advanced Materials and Manufacturing Technologies (AMMT) program and Transformational Challenge Reactor (TCR) program funded by the U.S. Department of Energy, Office of Nuclear Energy under Contract DE-AC02-06CH11357
- The authors gratefully acknowledge financial support from Argonne's LDRD SWIFT program 2021-0217
- This research used resources of the Advanced Photon Source, a U.S. Department of Energy (DOE) Office of Science User Facility operated for the DOE Office of Science by Argonne National Laboratory under Contract no. DE-AC02-06CH11357
- The authors thank Edward Listwan and Joe Listwan for their assistance with the experimental effort